

# Observations of Variability and Repeatability in Jointed Structures

M. R. W. Brake<sup>a,\*</sup>, C. W. Schwingshackl<sup>b</sup>, P. Reuß<sup>c</sup>

<sup>a</sup>*William Marsh Rice University, 6100 Main St., Houston, TX 77005, USA*

<sup>b</sup>*Imperial College London, South Kensington Campus, London SW7 2AZ, UK*

<sup>c</sup>*Daimler Automotive Group, Mercedesstraße 137, Stuttgart 70327, Germany*

---

## Abstract

The experimental study of joint mechanics has been limited in its effectiveness due to the high uncertainty associated with assemblies of sub-components. In particular, two categories of uncertainty are variability (the uncertainty in measurements of different, nominally identical parts) and repeatability (the uncertainty in measurements of the same set of parts). As a result, the uncertainty measured is often greater than the nonlinear characteristics being studied (such as amplitude dependent frequency and damping), which makes meaningful experimentation challenging. This paper analyzes the contributors to uncertainty in the form of variability and repeatability in order to make recommendations for methods to reduce the uncertainty and to redesign a joint to improve its dynamics. Experiments are summarized that investigate the role of experimental setup, interface roughness, settling versus wear, interface geometry (both meso-scale and macro-scale), and the structure surrounding the joint. From the results of these studies, recommendations for the measurement of nonlinearities in jointed structures are made.

*Keywords:* Joint Mechanics, Nonlinear Dynamics, Experimental Variability, Experimental Repeatability, Contact Mechanics, Tribomechadynamics

---

## 1. Introduction

One challenge in making meaningful predictions for the dynamics of jointed structures is that measurements of jointed assemblies exhibit a high degree of uncertainty. This uncertainty is in terms of both variability and repeatability, which have come to refer to two specific quantities within the joints community (Segalman et al., 2010; Starr et al., 2013). In this work, variability is used to refer to the intrinsic, part-to-part differences observed in measurements of nominally

---

\*Corresponding author; brake@rice.edu.

identical assemblies, and repeatability is defined as the measurement-to-measurement differences observed in experiments on the same assembly.

The high variability observed in jointed specimens includes variations in stiffness of 25% and damping of 300% for typical applications (Segalman et al., 2009). This could be due to wearing in, galling, alignment issues, changes in the microstructure, residual stresses, or some other phenomenon that is not evident at the macroscopic (or mesoscopic) view of the joint (for examples of these effects, see (Segalman et al., 2009; Brake, 2017; Catalfamo et al., 2016; Gianola et al., 2006; Prasad et al., 2011; Ren et al., 2016; Filippi et al., 2004; Kartal et al., 2011; Flicek et al., 2016)). Thus, a central question for the analysis of jointed assemblies is: what information is necessary to make accurate *predictions* (as opposed to calibrated simulations) about the dynamics of an assembled structure? In the extreme case, knowledge of the nano- and microstructure of an interface (detailing asperities, grain boundaries, etc.) will be necessary. If this is the case, prediction of the nonlinear dynamics of a jointed assembly *a priori* may be prohibitively difficult as the microstructure cannot be characterized before fabrication (for a typical specimen), and the microstructure is likely to change throughout experiments (Panzarino et al., 2016).

In real applications (i.e. not the carefully controlled academic experiments), this challenge becomes even greater. Due to manufacturing tolerances, nominally identical<sup>1</sup> (or nominally flat) specimen often have significant differences at the meso-scale that are not apparent without intensive inspection (Pesaresi et al., 2017). As an example, consider the samples studied in Chapters 9 and 12 of (Segalman et al., 2009), analyzed in depth in (Wang and Mignolet, 2014) and Chapter 35 of (Brake, 2017), and summarized in Fig. 1. At the interface, small variations in the meso-scale curvature due to manufacturing variability led to several fundamentally different contact pressure measurements. In turn, when part C was used in an assembly, the measured stiffness was relatively insensitive to the peak force amplitude, which was in sharp contrast to parts A and B. Thus, it is evident that features within a joint that modify the interfacial contact pressure must be accounted for in predictive numerical modeling.

This raises the question: what mechanisms drive changes in the interfacial contact pressure of a joint? The answers to this question in the literature are unsatisfactory. In part, this is due to a lack

---

<sup>1</sup>Throughout this paper, “nominally identical” is used to indicate that the specimens are designed to be identical, but due to the manufacturing process have variations that are within the specified tolerances for the design.

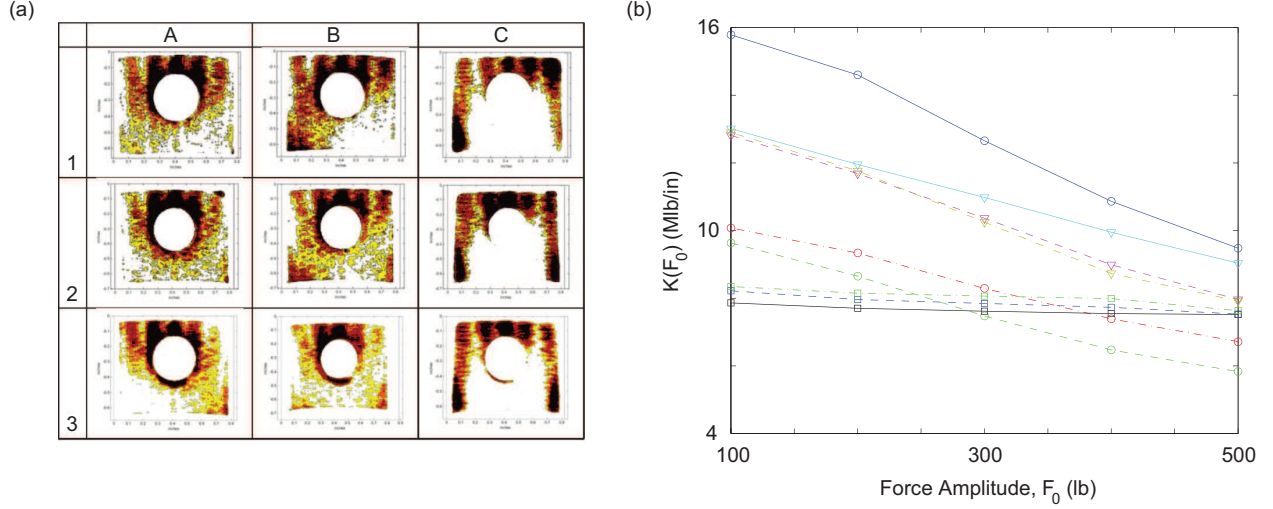


Figure 1: (a) Measured interfacial contact pressures and (b) stiffness versus peak force for nine nominally identical samples (from (Segalman et al., 2009)). Bottom parts A ( $\circ$ ), B ( $\nabla$ ), and C ( $\square$ ) denoted by symbols; top parts 1 ( $—$ ), 2 ( $- -$ ), and 3 ( $- \cdot -$ ) denoted by lines.

of understanding of friction in jointed assemblies - friction within a joint is poorly understood other than that Coulomb friction is not appropriate (Gaul and Nitsche, 2001; Ferri, 1995). This lack of understanding can be partly attributed to the multiscale nature of interfacial mechanics for jointed structures. Demonstrating this, the taxonomy of potential sources (Fig. 2) range from macro-scale geometry and loading to nano-scale grain boundaries. At the nano-scale, interfacial contact has been shown to drive grains to grow (or shrink in the case of large grains) in size (Panzarino et al., 2016). As evidenced by the formation of new grain boundaries, the nanostructure of an interface is highly variable throughout the life of a component. From a material perspective, contact mechanics is concerned (amongst other things) with the measurements of hysteretic behavior for specific material pairs<sup>2</sup> (Schwingshackl et al., 2012; Mulvihill et al., 2011b; Kartal et al., 2011; Filippi et al., 2004; Lavella et al., 2013; Cabboi et al., 2016). At the micro-scale, tribological studies have focused on the role of asperities (Mulvihill et al., 2011a) and mean roughness of a surface (Paggi and Barber, 2011; Putignano et al., 2011; Eriten et al., 2011) on an interface's frictional behavior. These studies have shown that knowledge of the actual contact area of an interface is paramount to understanding the frictional behavior. Meso-scale features, such as curvature, waviness, and machine tool patterns

<sup>2</sup>Particularly when measured hysteresis loops for a specific material pair and operating environment are used as direct input to the system level models that the cited researchers were charged with developing.

from the fabrication process may have an even greater effect on the development of the contact patch in an interface and the subsequent energy dissipation (see, for instance, (Müller and Ostermeyer, 2007; Seeger et al., 2018; Lawal et al., 2018)). Detailed analysis of the contact patch *in situ* (Seeger et al., 2018) highlights that deviations from flat surfaces significantly influence the contact pressure and normal loads within a joint. This, in turn, has a significant influence on the contact model (Cigeroglu et al., 2007) and dynamic behavior (Schwingshackl, 2017).

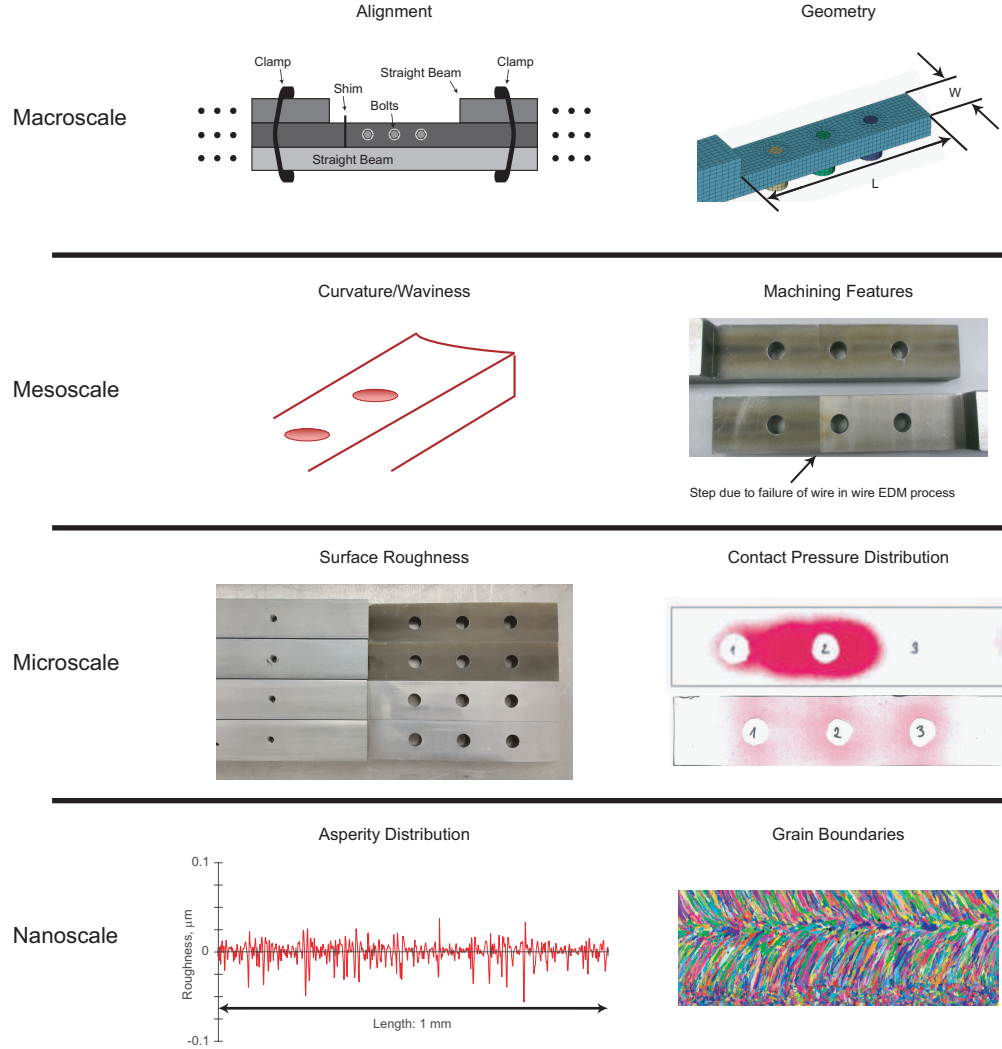


Figure 2: Examples of influences of variability/repeatability at multiple length scales.

As a result, experimentation becomes challenging if the multiple sources of uncertainty in terms of variability and repeatability are not properly controlled for (see, for instance, (Brake et al.,

2014; Brake, 2017)). Without a method to maximize the repeatability of an experiment, the characterized uncertainty is too high to be useful for meaningful numerical analysis. The practical ramifications of this lack of repeatability is starkly manifested in applications such as aeroturbines (i.e. jet engines). Each time an aeroturbine is reassembled following maintenance, the dynamic behavior of the aeroturbine dramatically changes due to the low assembly-to-assembly repeatability. Consequently, prediction of the remaining life of the aeroturbine is severely hampered, making structural health monitoring difficult and optimal maintenance scheduling infeasible since most of the previously collected response data is rendered useless by the low repeatability.

In what follows, the findings of a detailed, multi-year study of a system containing a single lap joint is discussed in order to provide new insights into the experimental attributes and geometrical features that can be controlled to reduce variability and increase repeatability in the dynamic response of jointed structures. this study emphasizes the importance of **Tribomechadynamics** (the integration of tribology, contact mechanics, and structural/nonlinear dynamics) in characterizing and designing jointed structures.

The specimens for this research are detailed in Section 2. These specimens are used to study the effect of the experimental setup in Section 3, and then to investigate the sensitivity of the response to settling effects/fretting wear (Section 4) and surface roughness (Section 5). Modified versions of the specimens are then used to investigate changing the geometry of the interface (Section 6) and changing the structure surrounding the joint (Section 7). The consequences of the results from the experiments are discussed in Section 8, and Section 9 summarizes the major conclusions of this paper. Note that due to the length of this study (spanning several years), many of the specimens used in the first few years of these experiments are unavailable for follow-on testing to fill in gaps in the data. Thus, general observations are made from the first two years of these measurements, which are then used to improve the testing procedure on the specimen used in the second half of the study (which includes specimen similar to those from the first years).

## 2. Nominal System

The focus of the present research is the Brake-Reuß beam, which is a benchmark structure for studying nonlinear dynamics in jointed systems that is currently being studied by approximately 20 institutions in the US and Europe (Brake, 2017). The Brake-Reuß beam is a 2.54 cm square cross-section beam consisting of a three bolt lap joint in the middle, as shown in Fig. 3 and the

appendix. Here, the Brake-Reuß beam is fabricated from 304 stainless steel; however, throughout the length of this study, the heat treatment and fabrication of the stock material was found to vary significantly. To control for this, each set of experiments details a group of specimen made from the same batch of stock material. Throughout this paper, multiple permutations of the Brake-Reuß beam are used to experimentally assess the influence of different features of a joint. Unless otherwise stated, the design of each specimen studied is identical to the nominal system described here.

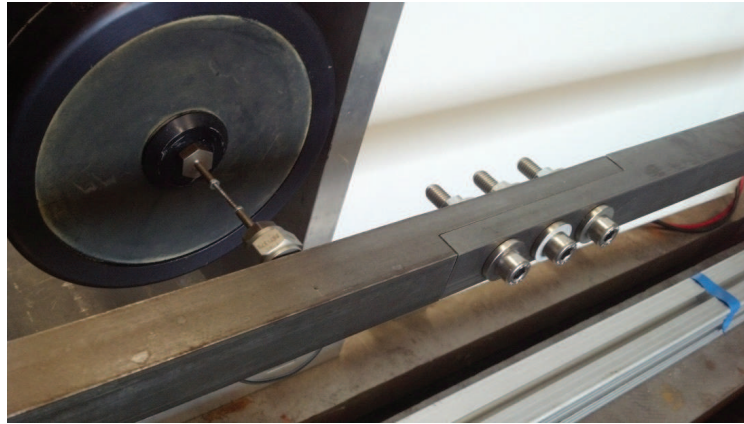
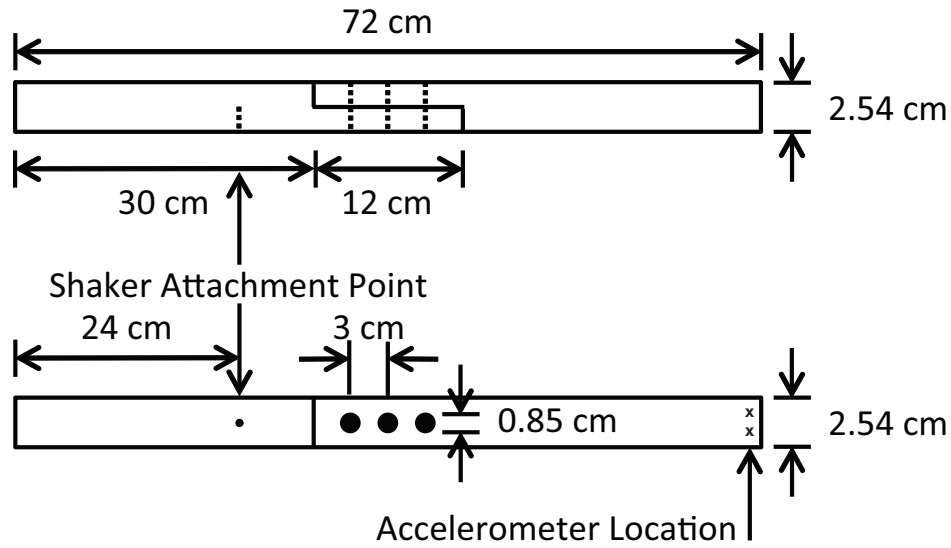


Figure 3: The geometry of the Brake-Reuß beam.

In the following experiments, the system is excited either via an impact hammer striking it at the same location as the shaker attachment point or an electromagnetic shaker (each experiment

detailed will specify the method of excitation). Accelerometers are glued to the system at the tip of the beam on the opposite side of the joint from the impact/shaker attachment location (as close as possible to the corners of the beam). When the shaker is attached, a 10-32 stinger is used as thin stingers are observed to bend at high excitation amplitudes, unintentionally exciting the torsional vibration modes of the beam (see (Smith et al., Under Review) for a discussion of use of different stingers). The 10-32 stinger is directly threaded into a force transducer, which, in turn, is connected to the beam by a 10-32 screw (see the engineering drawing in the appendix). The support structure around the beam has been constructed to minimize nonlinear effects introduced by boundary conditions (Smith et al., Under Review). The system is suspended via fishing lines in order to approximate free-free boundary conditions.

### 3. Variability and Repeatability Due to the Experimental Setup

#### 3.1. Overview of Preliminary Experiments

The first investigation of the Brake-Reuß beam is detailed in (Brake et al., 2014). In this investigation, a preliminary testing of the Brake-Reuß beam was conducted in order to evaluate the Brake-Reuß beam’s potential as benchmark system. Here, the primary conclusions are repeated in order to put the later experiments into context. The experiments of (Brake et al., 2014) primarily focused on the role of bolt tightening order (as the bolt tightening order influences the residual stress patterns in the interface – see Section 5) on repeatability in measurements of the system’s frequency response function during swept sine excitations via an attached shaker. Only one set of Brake-Reuß beams were fabricated for these initial experiments, which results in only repeatability being studied and not variability (which would require multiple systems to test). For all of the preliminary experiments, the shaker was attached away from the beam’s center line in order to excite torsional modes.

Three general observations were made. **First, higher repeatability was observed at low frequencies than at high frequencies.** This is evidenced both by the differences in repeatability observed in Fig. 4 and Fig. 5 as well as by similar results reported in (Brake et al., 2014).

**Second, increasing the preload led to higher repeatability.** This second observation was to be expected as a higher preload results in less motion across the interface. What was unexpected, though, was the extent of the lack of repeatability observed in many of the experiments. In Fig. 4, the nominal system of Fig. 3 was assembled and disassembled multiple times. Three different bolt

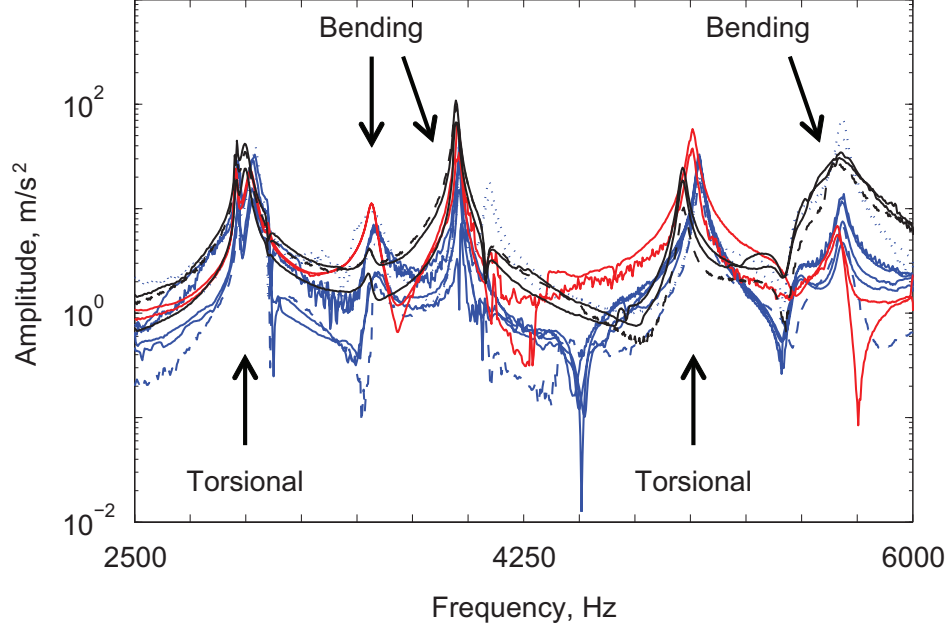


Figure 4: Frequency response function for the jointed beam with bolts tightened to a preload of 20 Nm. The different color lines correspond to different orders in which the bolts were tightened, and the (—) and (---) lines correspond to different assemblies of the system under the same conditions from the experiments of (Brake et al., 2014). Here, a high frequency range is shown in which the low degree of repeatability is particularly pronounced.

tightening orders were investigated: from left to right, middle then outside, and outside then middle. In each configuration, the bolts were tightened to 20 Nm with no intermediate tightening. Over the measured frequency range, the natural frequencies and damping ratios of each of the modes was observed to vary significantly (approximately 2-3% for stiffnesses and an order of magnitude for damping ratios). By changing the bolt tightening order, both numerical studies (Flicek et al., 2016) and experimental investigations (Catalfamo et al., 2016) show that the residual stress and distribution of contact pressures in the interface change significantly.

**Third, the bending modes and torsional modes in the system exhibit different sensitivities (in terms of repeatability to the bolt tightening order.** Figure 5 indicates that the bending modes (near 1200 and 1700 Hz) exhibit very high repeatability, while the torsional mode (near 1550 Hz) exhibits very low repeatability<sup>3</sup>. The torsional modes appear to be more sensitive to the interface conditions (including alignment) than the bending modes. It is unclear if this is an intrinsic property of the torsional modes of this system, experimenter induced error, or

<sup>3</sup>Similar trends are present in Fig. 4, but not discussed here for brevity.

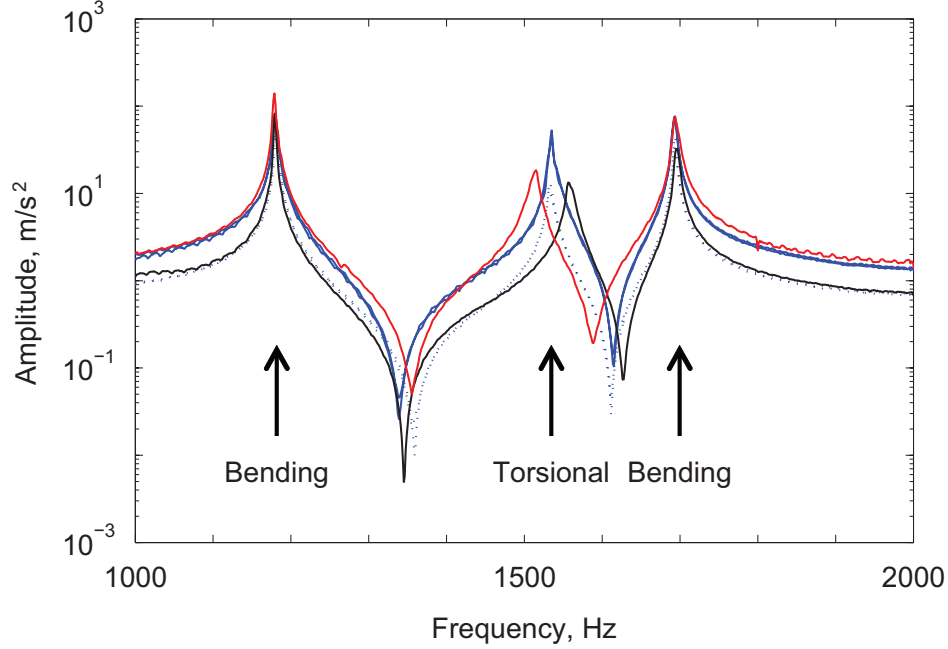


Figure 5: Frequency response function for the jointed beam with bolts tightened to a preload of 5 Nm. The different color lines correspond to different orders in which the bolts were tightened, and the (—) and (---) lines correspond to different assemblies of the system under the same conditions from the experiments of (Brake et al., 2014). The third and fourth bending modes are near 1180 Hz and 1690 Hz. The first torsional mode is near 1520 Hz.

something else. Thus, this highlights the need to remove as much experimenter-induced uncertainty from the experiments as possible in order to ascertain the true behavior of the system.

Following this preliminary study (Brake et al., 2014), a more thorough analysis of the system and its setup was undertaken, which is described in what follows. The observations presented from the preliminary study are similar to other studies of jointed structures (Segalman et al., 2009).

### 3.2. Measurements Using a Standardized Experimental Setup

From inspection of previous studies on jointed structures (Segalman et al., 2009; Brake et al., 2014; Smith et al., 2015; Catalfamo et al., 2016), there are multiple potential sources of uncertainty in the measurement of structural properties - surface roughness (i.e. micro-scale surface features), machining imperfections (i.e. meso-scale surface features), and misalignments and variations in bolt torque (i.e. macro-scale system features) amongst other sources. In controlling for micro-scale and meso-scale surface features (at least, to the best of the authors' ability to control these features), significant variability was still observed in the measurements of the structural properties (Smith et al., 2015). Subsequently, the hypothesis is put forth that much of the observed variability or lack

of repeatability can be attributed to the experimental error introduced by inconsistencies with the experimental setup. That is, for an experimental setup that is not sufficiently well controlled, attributions of variability (i.e. uncertainty in the part-to-part measurements) or repeatability (i.e. uncertainty in the assembly-to-assembly measurements) are convoluted with uncertainties introduced by the experimental setup.

In previous analyses of jointed structures, many attempts were made to standardize the experimental setup (Brake et al., 2014; Smith et al., 2015; Catalfamo et al., 2016); however, it was not intuitive as to which variables needed to be controlled in order to minimize variability (or maximize repeatability) of the experimental setup, resulting in reports of high variability in the system. Previous experimental setups (such as (Smith et al., 2015; Segalman et al., 2009)) convoluted the uncertainty due to nano- and micro-scale phenomena with the uncertainty due to the experimental setup. To address this issue, a series of experiments were conducted in order to determine a method to maximize repeatability due to the experimental setup. If successful, the remaining uncertainty in the measurements would be due to the actual variability of the system.

In what follows, the first three bending modes of the system are analyzed for a bolt torque of 20 Nm. The torsional modes are intentionally neglected here in order to focus the analysis on one phenomenon at a time; inspection of the result of the final experimental setup on the torsional modes is revisited later. Over the course of the four years that these experiments were conducted (Brake et al., 2014; Smith et al., 2015; Catalfamo et al., 2016; Dossogne et al., 2017), the system itself changed slightly. For each year of experiments, a new series of beams were fabricated. For the preliminary experiments of the previous section, the beams were fabricated in Germany, and thus conformed to metric units (i.e. their cross section was 2.5 cm instead of 2.54 cm). In subsequent experiments, the beams were fabricated in the United States, and the number of shaker attachment points were varied (in order to excite both on-axis and off-axis, and to excite at different driving points along the length of the axis). Consequently, the natural frequencies of the systems change slightly from experiment to experiment; however, the fundamental design of the system remained the same.

The experimental procedures investigated throughout this first series of experiments is summarized in what follows:

### 3.2.1. Procedure 1

The preliminary experiments on the Brake-Reuß beams described in the previous section was a scoping experiment to determine the suitability of the system for subsequent investigations (in terms of the presence/strength of nonlinearities and the variability characteristics). From the preliminary experiments, the first experimental setup (Brake et al., 2014) controlled for:

- Bolt tightening order;
- Bolt preload (bolts fully tightened with no intermediate tightening);
- Interface alignment via resting the beams on a level surface and clamping together before tightening the bolts; and
- Excitation via shaker attached away from the beam’s center line to excite torsional modes.

In these experiments, one set of beams was studied. The natural frequencies were found to vary up to 5.6% (for the first three bending modes), and the damping ratios varied by an order of magnitude between different assemblies of the same system using identical test conditions. Two representative measurements are shown in Fig. 6, in which the order that the bolts were tightened was varied. As previously mentioned, the experiments in (Brake et al., 2014) exhibited low repeatability, and showed a significant influence of bolt tightening order on the measurements of natural frequency and damping ratios for torsional modes. For bending modes, the bolt tightening order significantly influenced the damping ratios, but had a lesser (5.6%) influence on the natural frequencies. For 20 Nm bolt torques, the first torsional mode is close in frequency to the fourth bending mode (1685 Hz versus 1745 Hz respectively). Despite a consistent excitation location and method, the torsional mode was more prominent for some assemblies of the system than for others. In this first series of tests, the experiment-to-experiment repeatability for a specimen was too low for the nonlinear properties of the system to be characterized with confidence.

### 3.2.2. Procedure 2

The second experimental setup (Smith et al., 2015; Catalfamo et al., 2016) is from the first two years of the Nonlinear Mechanics and Dynamics (NOMAD) Research Institute (Brake et al., 2015, 2016) in which the applicability of linear experimental techniques for measuring nonlinear system properties are assessed. This experimental setup controlled for:

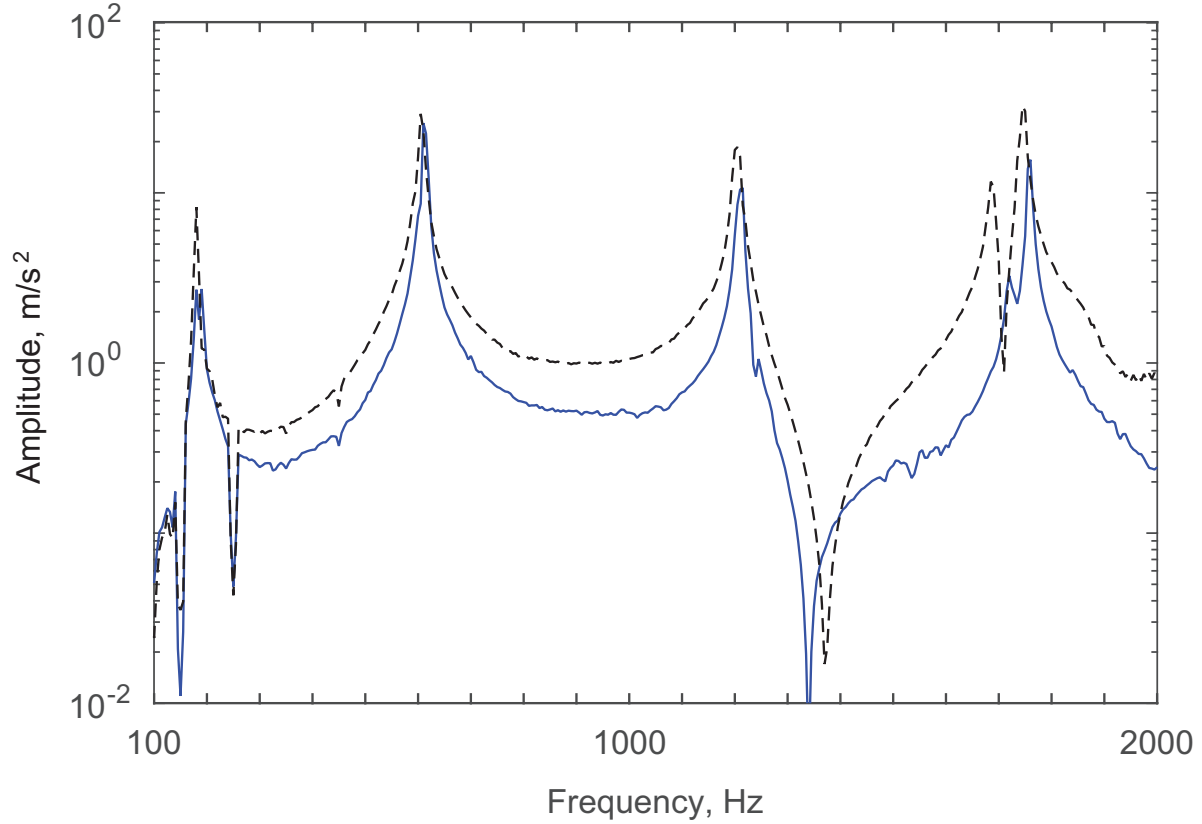


Figure 6: Frequency response function for the jointed beam with bolts tightened to a preload of 20 Nm for the first experimental procedure. Shown are representative responses for tightening the bolts left to right (—) and outside then middle (---). In both cases, the response to a low amplitude excitation is shown to highlight the linear frequencies of the system.

- Bolt tightening order;
- Bolt preload (all bolts are tightened to half of the prescribed torque in order, then to the full torque in the same order);
- Interface alignment via clamping the beams to a nominally straight beam; and
- Excitation via shaker attached on the beam's center line to avoid exciting torsional modes.

This set of experiments primarily investigated the role of interface roughness on measured dynamic properties of a jointed system. Ten separate pairs of beams were studied, two each of five distinct

roughness levels. In assessing the repeatability of these beams<sup>4</sup>, Fig. 7 shows a clear difference between the dynamic behavior of one of the rough beams (with a mean surface finish of 2.0  $\mu\text{m}$ , and response shown in Fig. 7(a) and (c)) and of one of the mirror-like beams (with a mean surface finish of 0.02  $\mu\text{m}$ , and response shown in Fig. 7(b) and (d)). **The beams with a mirror-like interface exhibited a significantly higher repeatability across assemblies than the beams with a rough interface** (which were approximately the same roughness as the beams fabricated for the experiments of (Brake et al., 2014)). This is evidenced by the wider spread of measurements for the rough beams as compared to the mirror-like beams. Further, the beams with mirror-like interfaces exhibited a repeatable measurement of frequency and damping ratio for all bolt torque levels greater than 3 Nm (in Fig. 7(b), all but the 3 Nm tests have a linear frequency around 185 Hz, and stiffness nonlinearities of similar strengths). The repeatability in frequency for the rough beam when excited via an impact hammer was measured to be 0.2% of the first natural frequency for a bolt torque of 15 Nm, which is approximately 4% of the variability measured in Procedure 1. The mirror-like beams, by contrast, exhibited a variability of 0.02% of the first natural frequency for a bolt torque of 15 Nm.

From studying the variability of the system via shaker excitation, the beams with mirror-like interfaces were not significantly influenced by the bolt tightening order in terms of the measured variability of the natural frequencies. For the beams with rough interfaces, the bolt tightening order did not appreciably affect the lower modes, but some variability was observed in the natural frequencies for modes above 2000 Hz. Of note, the change in resonant frequency as the response amplitude is increased was measured as approximately 1.5% of the natural frequency; this value is approximately 25% of the measured variability using Procedure 1. **Thus, this nonlinear behavior could not be accurately measured with Procedure 1.** These results are further discussed in Section 5, in which the role of contact pressure on variability is investigated.

### 3.2.3. Procedure 3

The third experimental setup is from the third year of the NOMAD Research Institute (Dossogne et al., 2017; Cooper et al., 2017), which investigated the roles of settling and wear, changing the interface geometry, and changing the far-field structure (as discussed in Sections 4, 6, and 7). This

---

<sup>4</sup>Unfortunately, no appropriate data from shaker measurements is available to highlight this set of experiments. Instead, impact hammer testing that was done at the same time is used to discuss the influence of the test setup.

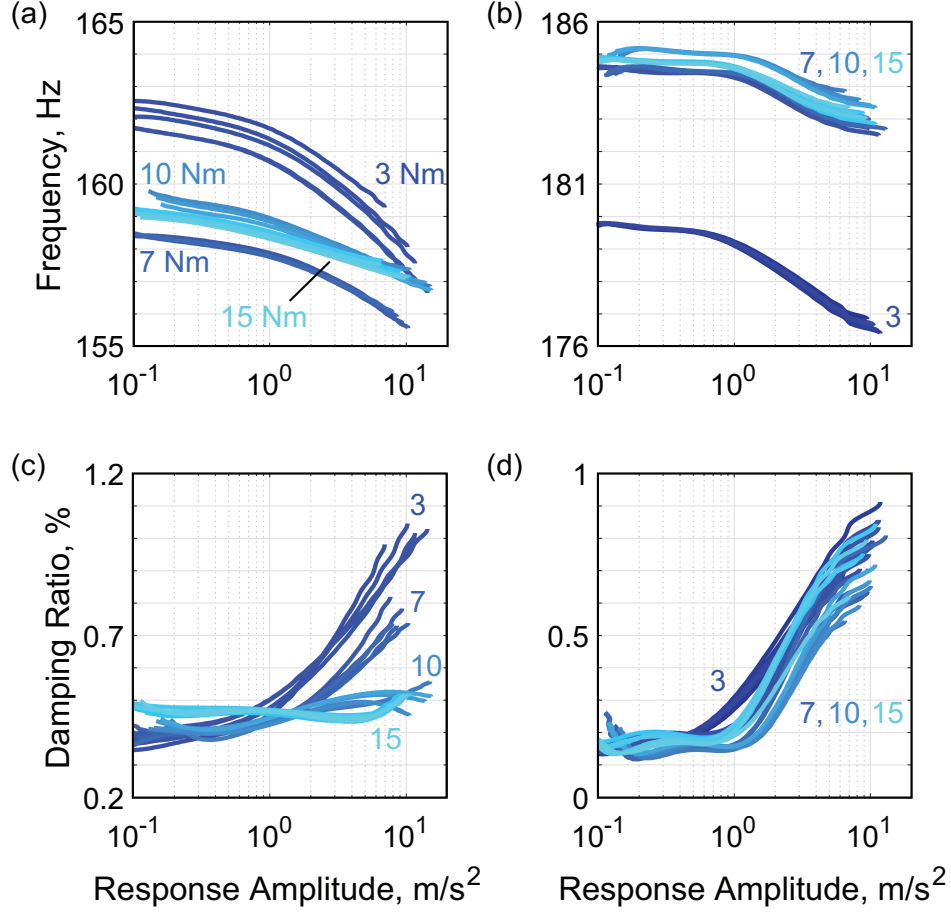


Figure 7: Amplitude dependent (a) and (b) frequency and (c) and (d) damping ratio for the jointed beam with (a) and (c) a mean surface finish of 2.0  $\mu\text{m}$ , and (b) and (d) a mean surface finish of 0.02  $\mu\text{m}$ . Shown are responses for bolt torques of 3 Nm (darkest), 7 Nm, 10 Nm, and 15 Nm (lightest), extracted from impact hammer tests of the system setup using Procedure 2.

final experimental setup controlled for:

- Bolt tightening order (outside then inside);
- Bolt preload (all bolts are tightened to 70% of the prescribed torque in order, then to the full torque in the same order);
- Interface alignment via clamping the beams between two nominally straight beams;
- Gap alignment via the use of a shim; and
- Excitation via shaker attached away from the beam's center line to excite torsional modes

(though tests with the shaker attached to the beam's center line were used for comparison to previous years).

This third experimental procedure differs from the previous two by being more rigorous in assuring that the interface is aligned the same way each time. Figure 8 highlights the alignment procedure: two sets of beams, one set of half beams above and one long beam below, are used to align the system in the plane of the interface (tightening the bolts aligns the system orthogonally to the interface). A shim is used to ensure that the gap between the portions of the lap joint parallel to the axis of the bolts is consistent with every assembly. The thickness of the shim is slightly wider than the wire used in the wire EDM manufacturing process for cutting the stock material into two separate beams (approximately 0.335 mm). The usage of two beams compared to one for aligning is a matter of convenience and not otherwise advantageous. This procedure tightened the center bolt to 70% of the prescribed torque values then each of the outside bolts to the same level. Once all three bolts had been tightened to this intermediate level, all three bolts were tightened fully in the same order. This methodology is in accordance with standard assembly procedures found throughout the motivating industries.

The frequency response of the first mode is shown in Fig. 9. Due to the high observed repeatability, the uncertainty between measurements is negligible, such that the effects of excitation levels can be clearly seen. This enables parameter studies to assign causality. Subsequently, very high resolution measurements were made for each mode. For the first mode, the variation in frequency was observed to be about 0.06% for each load level across three separate assemblies. As the load is increased, a decrease in the natural frequency of the system is observed, which is expected due to the activation of the nonlinear behavior. However, the decrease in natural frequency for the first mode as the excitation amplitude is increased from 0.1 N to 2.0 N is 1.25% of the natural frequency, which is smaller than the variability observed in previous setups. Thus, without proper control of the experimental setup procedure to ensure that variability is not introduced to the system due to alignment issues, the variations in the measurements due to variability and lack of repeatability are greater than the measurements of frequency shifts. **If a stochastic model of the system is more important than precisely understanding the nonlinearities in the system, then intentionally introducing uncertainty in the experimental setup would seem to span the extent of the nonlinear response for this system** (i.e. the nonlinear response would be

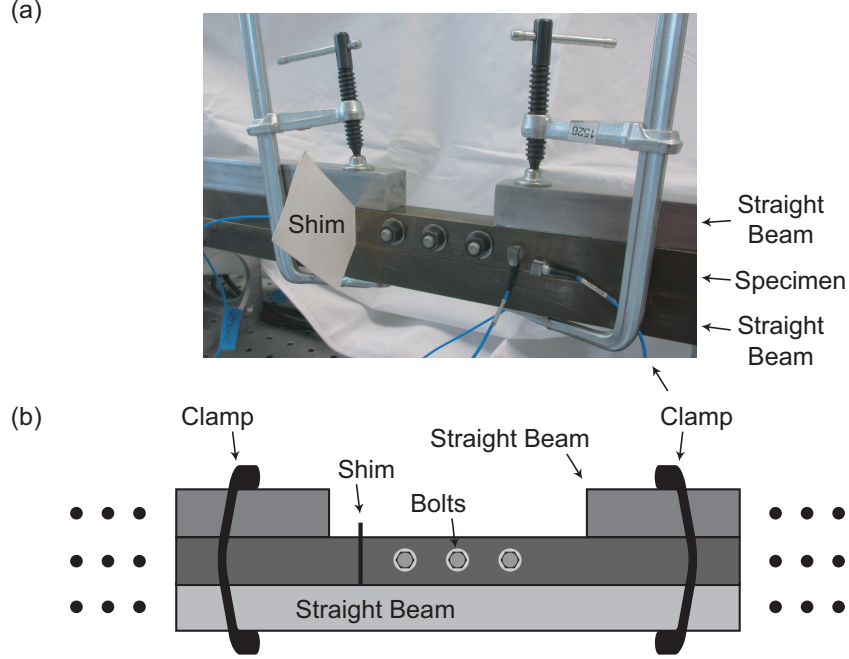


Figure 8: (a) Photo of the alignment technique used in the third procedure. (b) Illustration that highlights the alignment of the interface used for the third procedure.

overshadowed by the variability). In general, this has not been demonstrated as only one class of joints was investigated. Success in this type of approach was found in (Wang and Mignolet, 2014) for the joint of Fig. 1.

From analysis of the results from the three different testing procedures, there is support for the hypothesis that the degree of repeatability or variability in an experiment is directly related to how well the aspects of the experimental setup that influence the frictional interactions for an assembly are controlled for. Another way of framing this is in terms of the consistency of the experimental setup from one assembly to the next. By removing sources of uncertainty in the experimental setup, the remaining measured uncertainty is able to be attributed to the interfacial interactions. Thus, **in order to make meaningful conclusions about the dynamics of jointed structures, it is paramount that the experimental setup be carefully controlled.** While this conclusion may seem obvious, the insidious/zemblanitous nature of it is that many of the sources of uncertainty are often overlooked. This emphasizes the need for testing a control (linear) system first to establish that an experimental setup does not introduce nonlinear effects into measurements (for instance,

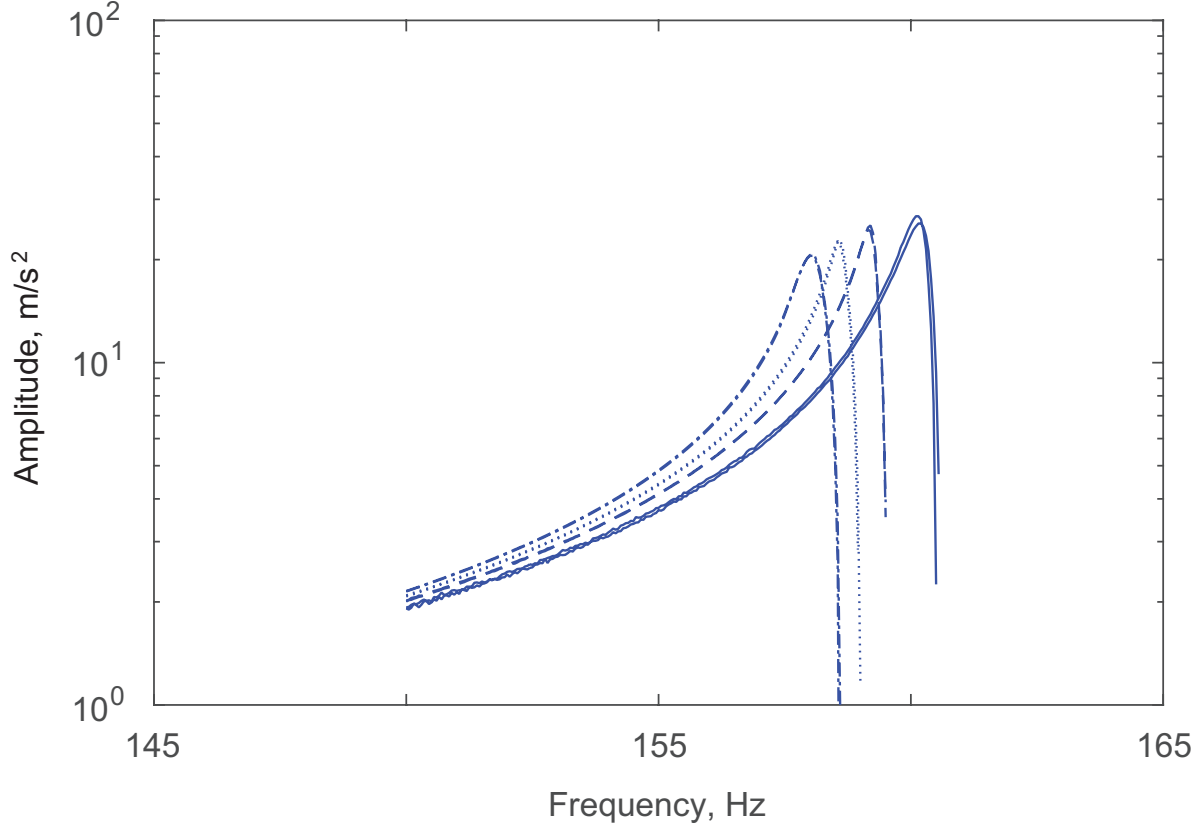


Figure 9: Frequency response function for the jointed beam with bolts tightened to a preload of 20 Nm for the third experimental procedure. Shown are responses near the first mode for excitations of 0.1 N (—), 0.5 N (– –), 1.0 N (···) and 2.0 N (– · –) across three assemblies.

see (Smith et al., Under Review)).

### 3.3. Excitation Methods

Consideration was given to the best excitation method for the system, with several different approaches investigated. The initial procedures used a shaker attached to the system via a 10-32 threaded stinger. The shaker was used to excite the system at both fixed frequencies and via a sine sweep. Both force and amplitude control were investigated. The latter was considered the better choice to investigate nonlinear dynamic behavior around resonance, as a constant amplitude during the stepped sine sweep leads to a constant activation of the joint. This results in similar contact behavior throughout the sweep, and, consequently, a linearized response for each sweep level. This linearization allows the use of standard linear modal analysis tools for data processing, thereby

reducing uncertainty in the processed data<sup>5</sup>. Unfortunately, the strongly nonlinear behavior of the joint, and the relatively high amplitude levels required for their activation, made this approach time consuming. As an alternative approach, force control was predominantly used. This led to an easier control of the system, but the changing response amplitude at the interface during a stepped sine sweep led to an increasingly stronger activation of the nonlinearities. Consequently, this method potentially introduced greater variability in the results due to uncontrolled settling events at the joint.

The large amplitude required for the nonlinear dynamic investigation of the joint necessitated a relatively stiff stinger connection between the shaker and the beam, leading to cross coupling effects at resonance. Unfortunately, the shaker had noticeable influence on the beam response, introducing further uncertainty into the response measurements. These considerations made shaker excitation less than ideal, and led to the adoption of impact hammer testing instead. An alternative approach, not explored here, would be to use the shaker to excite the system at resonance, then to decouple the shaker and specimen. In this manner, the free decay of the system can be measured as the system rings down (Noël et al., 2014; Peeters et al., 2011b,a); however, the mechanism to attach and decouple the shaker was not available for these experiments.

Impact hammer testing has several advantages and disadvantages compared to shaker excitation. As an advantage, it is able to provide broad band excitation of multiple modes in the system from a single test. After impact, the influence of the exciter is removed, and it allows the extraction of the nonlinear dynamic response at different amplitudes from a single ring down. As a downside, impact hammer testing of nonlinear dynamic structures requires advanced data analysis techniques to separate different modal contributions and study the amplitude dependent response of each mode. Impact hammer testing can lead to a more complex behavior at the interface due to the nonlinear coupling of multiple modes that have been excited by the impact hammer, and a repeatable excitation force is harder to achieve (in terms of magnitude, precise location, and angle of impact). As a result impact hammer testing reduces some of the variability from the shaker testing, but it introduces other potential sources of uncertainty.

---

<sup>5</sup>Due to the nature of the nonlinearities, as long as the experiments were well below the macroslip threshold, the mode shapes of the system remained approximately constant. Thus, there is reasonable confidence that the output of the accelerometer or force transducer is suitable for control of the excitation of the jointed interface.

### 3.4. Recommended Experimental Setup and Analysis Details

In the remaining experiments, the experimental setup of procedure three was used, but with impact hammer testing (excluding the settling versus wear study that follows). This allowed for measurement of the free decay of a system such that the amplitude dependent frequencies and damping ratios could be calculated. To calculate the amplitude dependent frequencies and damping ratios in the following sections, the measured transient responses are filtered about a single mode then analyzed using a Hilbert Transform (Dossogne et al., 2016, 2017; Allen and Mayes, 2010; Sumali and Kellogg, 2011; Feldman, 1994), and a polynomial function is fit to the amplitude of the ring-down response. From this fit, the amplitude dependent natural frequency and amplitude dependent damping ratio are extracted. These two quantities are then used to characterize the nonlinear dynamics of a jointed system.

Before each experiment, the assemblies are shaken down by a series of low amplitude impacts (less than 100 N) across the length of the beam, resulting in a more consistent result as the first several measurements after assembling a system tended to exhibit relatively low repeatability (this is hypothesized to be due to a new pattern of asperities being engaged that needed to be broken in).

The frequency responses of forty five impact measurements are shown in Fig. 10 (three assemblies, three excitation magnitudes, and five repetitions per condition). The variations observed in these measurements are not as low as for the shaker excitation (due to the intrinsic variations in the impact hammer strikes); however, the repeatability is significantly higher and the variability is significantly lower than found with the other testing procedures. Table 1 details the observed variations in frequency for each method. **One conclusion that can be drawn from these results is that much of the initially observed variation was due to the experimental setup. By properly controlling the experimental setup, the observed variations in the measurements are reduced by almost two orders of magnitude.** This leads to the Repeatability Hypothesis for joint mechanics:

**The Repeatability Hypothesis** states that the observed variation in the dynamic properties of a jointed specimen in sequential experiments is due to experimental error.

If this hypothesis is supported by further testing, then a consequence would be that experimental uncertainty/error can be calculated directly from the repeatability of a system. One important

caveat to the Repeatability Hypothesis is that systems that incur plastic damage, fretting fatigue, or other significant amounts of wear will exhibit permanent changes in the dynamic properties of the assembly. However, excluding a high amplitude event that may damage the interface, it is reasonable to expect that the measured dynamic properties remain constant in back-to-back (sequential) experiments. In the next section, the effect of damage is studied following a high amplitude excitation. Thus, repeatability is not to be expected due to the accumulation of damage from test to test.

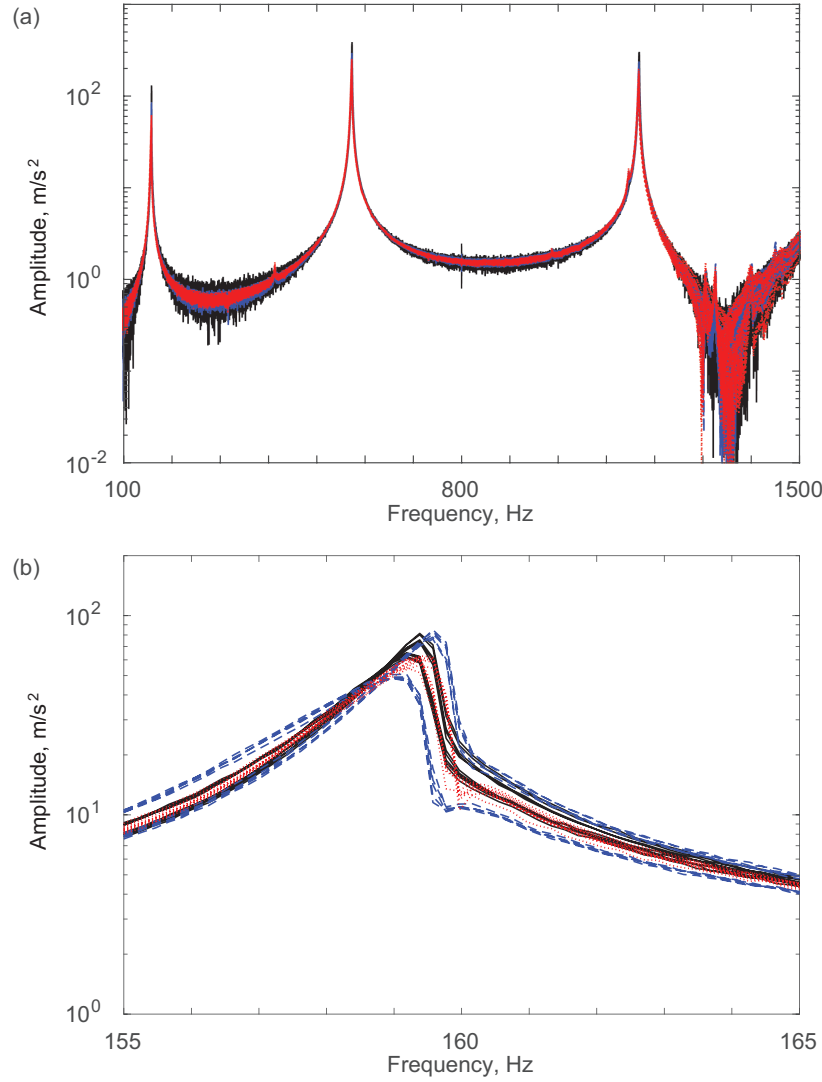


Figure 10: Frequency response function for the jointed beam with bolts tightened to a preload of 20 Nm for the third experimental procedure using an impact hammer for excitation showing (a) the first three bending modes, and (b) the first bending mode. Shown are responses for low (—, black), medium (---, blue), and high (···, red) impact forces.

	Procedure 1S	Procedure 2S	Procedure 3S	Procedure 3I
First Mode	5.6%	3.1%	0.063%	0.13%
Second Mode	2.5%	0.48%	0.052%	0.070%
Third Mode	3.3%	1.7%	0.085%	0.086%

Table 1: Measured repeatability (defined by the maximum difference in responses) in the natural frequencies of the first three modes for the procedures discussed in Section 3.2. The bolt torques (20 Nm), interface roughness (1  $\mu\text{m}$ ), and fixturing are held constant across all tests. Procedure numbers followed by an S refer to shaker testing, and the number followed by an I refers to impact hammer testing.

#### 4. Role of Settling and Wear

Even with the high repeatability achieved in the previous section, the natural frequency of the system has been observed to change over time across a series of experiments. Two hypotheses were put forward to explain this behavior. The first hypothesis is that the interface was settling, in which case the natural frequency would eventually converge to a single value and disassembly/reassembly would result in the natural frequencies being temporarily perturbed before returning to the converged value after settling again. The second hypothesis is that the system was incurring wear (even though it is subjected to very low cycle excitation), in which case visible damage on the interface would eventually manifest and the natural frequencies would be permanently decreased by each set of experiments.

To test these hypotheses, a study was setup in which the nominal system was subjected to a sine sweep over the first natural frequency by a shaker at 0.1 N. The shaker amplitude was increased to 0.2 N and the test was repeated. Following the 0.2 N test, the amplitude was decreased to 0.1 N, and the test was repeated again. The total set of amplitudes tested, in order, are: [0.1, 0.2, 0.1, 0.5, 0.1, 1.0, 0.1, 2.0, 0.1, 4.0, 0.1, 8.0, 0.1, 12, 0.1, 16, 0.1, 20, 0.1.] N. That is, every other test was at the low amplitude level, and the even tests increased in amplitude from 0.2 N to 20 N.

Figure 11 shows the results of this experiment for three separate assemblies (all on the same beam pair with bolt torques of 20 Nm). Several observations can be made. First, all measurements show a significant decrease in response amplitude with increases in excitation magnitude, and for the highest level tested (20 N), the responses appear to converge near 158.5 Hz with an amplitude of 3  $\text{m/s}^2/\text{N}$ . Surprisingly, this converged value is a *higher* frequency than the initial measurements for the second and third assemblies of the system.

The second set of observations is that the frequency and response amplitudes (indicating damp-

ing) of the low level excitation tests change dramatically from the start to the end of the experiment. For the first set of tests, the frequency shows a significant decrease from 160.75 Hz to 158.5 Hz. This change is above the measured variability previously reported for this experimental procedure. The second and third set of experiments show a smaller change in frequency (of only 1 Hz net). Similar results have also been found for other torque levels (15 Nm and 25 Nm) in which the frequency shifts were significantly larger than the previously observed experimentally measured variations. Not observed at other bolt torques is the increase in natural frequency for the second and third assemblies of the system at high excitation amplitudes. This implies that some settling does occur as disassembly and reassembly returns the system to the initially measured frequency (i.e. from the second to the third measurement).

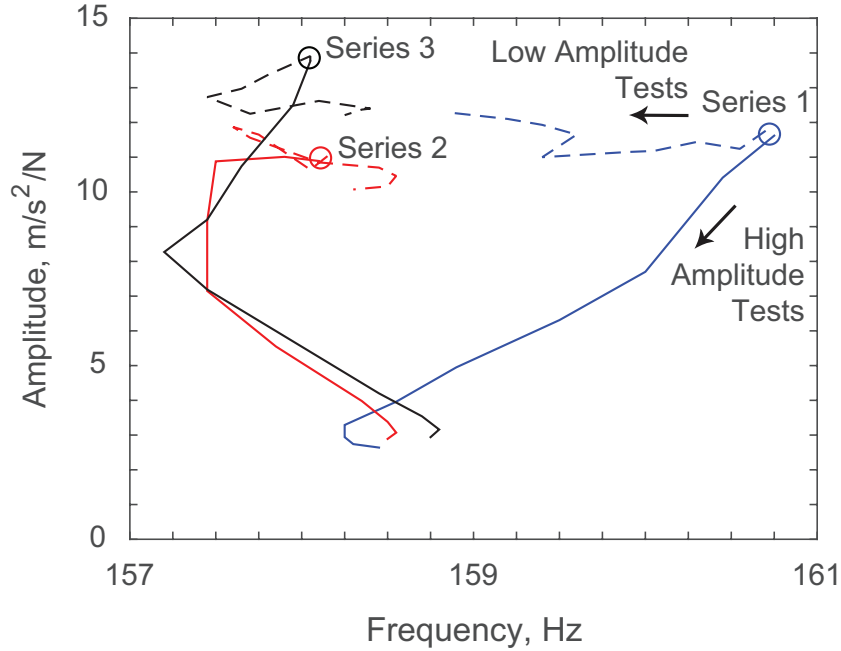


Figure 11: Evolution of the first natural frequency across three separate assemblies of the nominal system (blue, red, and black in order and indicated as 1, 2, and 3). The high amplitude excitation response is shown as (—), and the 0.1 N excitation response is shown as (---). The initial measurements for each assembly are indicated by circles.

After testing was completed, the interface was inspected for damage. In Fig. 12, visible pitting and fretting wear was observed on the interface near the areas of low contact pressure (both as measured via pressure film (Dossogne et al., 2017) and as predicted by numerical simulations (Lacayo et al., 2017)). **This finding leads to the conclusion that the observed initial change in natural frequency over time is due to wear in the interface.** The rate of

change of the natural frequencies decreased after the initial set of experiments; however, continued testing of the beam (see (Scheel et al., 2018) for results from the same beam a year later in which natural frequencies as low as 145 Hz were measured) has found that the natural frequencies have not yet reached a lower limit. Unlike many systems that experience wear and fretting fatigue due to high cycle loading (Flicek et al., 2015), this system was only subjected to low cycle loading. Further investigation (Seeger et al., 2018) shows that the portion of the interface that has low contact pressure under static loading undergoes a cyclic behavior under dynamic loading in which the contact pressure dramatically changes during the course of a period of excitation, and a gap at the edge of the interface is achieved with the nominal bolt torque of 20 Nm leading to a clapping behavior. This dynamic evolution of the contact pressure in the interface is most likely the source of the low cycle fatigue observed in this system.



Figure 12: Photo of pitting on the interface surface after the settling/wear study.

It is worth noting that these wear issues are also observed during impact hammer excitations, but only once the force magnitude has been sufficiently high enough to initiate either macroslip or subsurface yielding in the interface (the force needed to incur damage in this system from impact hammer testing has been observed to be on the order of 10 kN) (Bonney et al., 2016). Once the system has incurred damage, each subsequent experiment has been observed to further damage the beam. This is evident in the permanent shifts in natural frequency that are observed for shaker excitation magnitudes as low as 0.2 N. It is likely that even low cycle fatigue is unavoidable for this system with shaker excitation except at the lowest force levels possible. Thus, in order to minimize observed variability due to wear, impact hammer testing is recommended and is subsequently used in what follows.

The major conclusion of this section is that while the system may have experienced some

settling, the observed shifts in natural frequency for low amplitude excitations was due to fretting wear of the interface. This was confirmed through both visual inspection of the interface and the permanent (and continued) reduction in natural frequency observed across a series of experiments.

## 5. Variability and Repeatability Due to the Roughness

Revisiting the role of interface roughness, a follow-on experiment was conducted in (Bonney et al., 2016) to develop uncertainty distributions for the set of parameters describing lap joint models. In these experiments, the bolts were tightened to a prescribed level (ranging from 3 Nm to 15 Nm), and Procedure 2 was followed (as this study occurred at the 2015 NOMAD Research Institute), with the exception that impact hammer excitation was used instead of a shaker. Figure 7 shows the amplitude dependent natural frequency and damping ratio for the first mode of two different beam: one with a 2.0  $\mu\text{m}$  mean roughness (Fig. 7(a) and (c)), and one with a 0.02  $\mu\text{m}$  mean roughness (Fig. 7(b) and (d)). These values are extracted from the ring down response of the system using a Hilbert transform after the data has been filtered for a specific mode (here, the first mode) (Dossogne et al., 2016). For linear systems, the amplitude dependent frequency and damping ratio are straight (horizontal) lines. The amount that these quantities deviate from a straight line indicates how strong the nonlinearity in the system is for the filtered mode. In a typical lap joint, the natural frequency decreases with excitation amplitude (indicating softening behavior as more of the interface is in slip), and the damping ratio increases with excitation amplitude (indicating more energy being dissipated as more of the interface is in slip).

Figure 7 shows several trends. **First, as the bolt torque is tightened on the smooth interface, the response saturates.** That is, for all bolt torques of 5 Nm and higher, the natural frequency of the system converges to a linear frequency of 185 Hz with similar stiffness nonlinearities (i.e. how much the natural frequency changes with response amplitude), and the damping ratios are identical for all tests. This is not the case for the rough interface, however.

Second, **for each torque level** (indicated by a set of five measurements at a different shade of blue, dark corresponding to 3 Nm and light corresponding to 15 Nm), there is significantly more variation in the measured properties for the rough interface than for the smooth interface. That is, for the beams with high roughness, the repeatability is observed to be low. By contrast, and similarly to the Procedure 2 experiments, the 0.02  $\mu\text{m}$  roughness beams exhibit high repeatability as indicated by the narrow cluster of lines in Fig. 7(b) and (d).

The measurements of uncertainty due to the interface roughness are partially explained by analyzing the measured contact pressure in the interface of each assembly. In Fig. 13, static contact pressure film is used to measure the interfacial contact pressure for both the rough and smooth interfaces under different bolt torques and for different bolt tightening orders. The measurements show that the interfacial contact pressure for the smooth interface is relatively insensitive to the bolt tightening order. By contrast, the interfacial contact pressure for the rough interface is significantly different for each assembly. As the location of regions with high contact pressure changes and as the areas with relatively little contact pressure changes (indicating a higher potential for microslip) from assembly to assembly, this results in much of the observed uncertainty, and has been further confirmed through numerical analysis (Lacayo et al., 2019).

Specifically, in the context of these experiments, when there is a high, uniform contact pressure, lower variability is observed than when the contact pressure in the interface varies significantly and includes large areas with low contact pressure. Here, the contact pressure measurements for the rough beams indicate that there are several small regions of high contact pressure, but most of the interface is characterized by low contact pressure between the two mating surfaces. In the next section, the contact pressure in the interface is intentionally changed through the redesign of the meso-scale and macro-scale geometry of the interface.

To control the variability and repeatability in the results for future investigations, a roughness of  $0.1\text{ }\mu\text{m}$  is used in what follows. This roughness level has been found to have consistent interfacial contact pressure measurements and is significantly easier to manufacture than the mirror-like finish used in the roughness study described above.

## **6. Influences of Meso- and Macro-Scale Features on Variability and Repeatability**

Following the analysis of the experimental setup and the influence of surface roughness on variability and repeatability, the next study focused on the influence of meso-scale and macro-scale interface features. The subsequent experiments fall into two categories: first, the changing of the meso-scale geometry of the interface through modification of the curvature of each side of the interface, and second, the changing of the macro-scale geometry of the interface through the introduction of geometric features designed to change the shape of the contact patch.

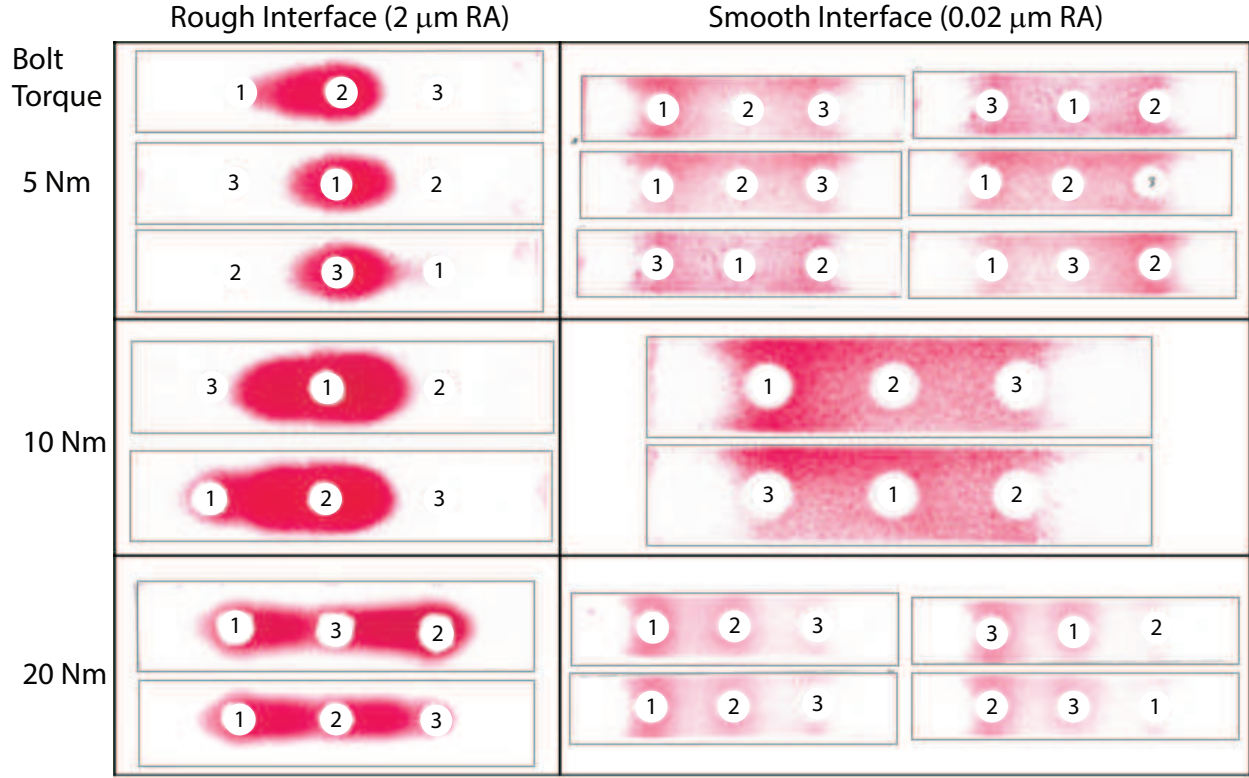


Figure 13: Static contact pressure film measurements made for both smooth and rough interfaces at different bolt torques. The order in which the bolts were tightened is indicated numerically for each measurement. For all measurements, each set of bolts were tightened 50% then to 100% of the prescribed bolt torque.

### 6.1. Meso-Scale Interface Variations

The first set of interface modifications focused on the introduction of curvature to the interface. As real systems may have unintended meso-scale features from the manufacturing process, the curvature modifications are intended to provide some insight into how local curvature effects influence the dynamics of the jointed system. Five different curvature heights, defined in Fig. 14, were manufactured: 0 (the nominal system), 50  $\mu\text{m}$ , 250  $\mu\text{m}$ , 1000  $\mu\text{m}$ , and 5000  $\mu\text{m}$  (see (Lawal et al., 2018) for the details of manufacturing these beams). Curvatures of 5000  $\mu\text{m}$  are not expected to be the result of typical manufacturing errors; however, this case is of interest as an extremum for this experimental study.

The curved interfaces are assembled in three different configurations. The conformal configuration (Fig. 14(b)) is defined as the two matching beams being mated together. The center gap

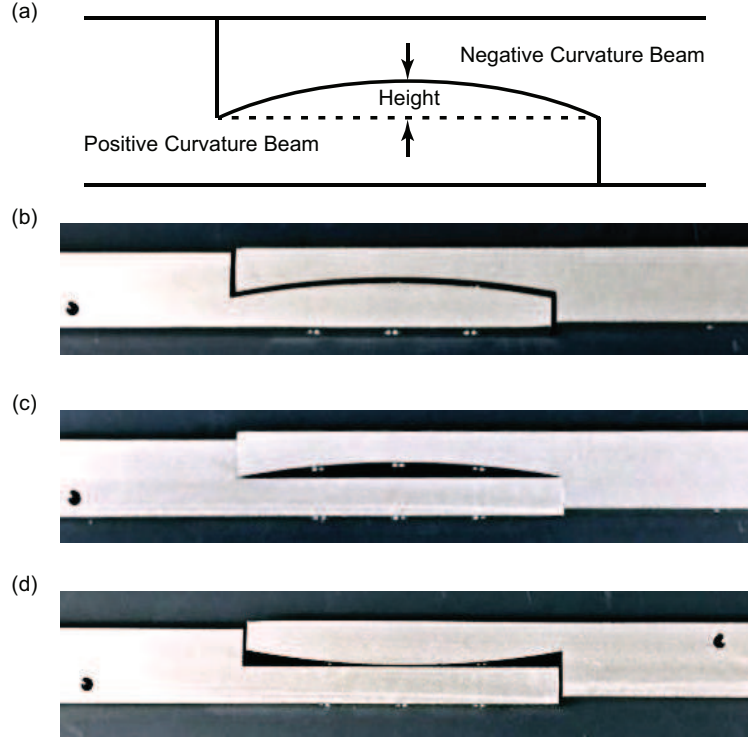


Figure 14: Modifications of the interface curvature of the Brake-Reuß beam showing the (a) drawing of the definition of curvature in terms of the height of the deviation from being flat, (b) image of the conformal condition, (c) image of the center gap condition, and (d) image of the edge gap condition.

configuration (Fig. 14(c)) is defined as a negative curvature beam mated to a nominally flat<sup>6</sup> beam, which results in a gap in the center of the interface. Last, the edge gap configuration (Fig. 14(d)) is defined as a positive curvature beam mated to a nominally flat beam, which results in gaps at the edge of the interface. As the curved beams are designed such that the beam's center line passes through the center of the curvature, both the edge gap and center gap configurations result in an assembly that are no longer the same height as the nominal system (as shown in Figs. 14(c) and (d)). Because of this, the center gap and edge gap configurations are only investigated for small curvature heights.

## 6.2. Influence of Meso-Scale Interface Variations on Variability and Repeatability

Using test procedure 3I, impact hammer tests were performed on the curved interface assemblies for each of the configurations. The measured amplitude dependent frequency and damping ratio

<sup>6</sup>Here, “nominally flat” is intended to indicate that the beam is intended to be flat, but in reality it has some non-zero curvature of its own.

are shown in Fig. 15 for 600 N impacts (within a  $\pm 5\%$  range) with bolts tightened to 19.6 Nm. Each curve in Fig. 15 is the average of 15 measured responses from three assemblies of the same system. To average the response, a spline interpolation was performed in Matlab to calculate the trend line for all 15 measurements. The variability in the responses was observed to be similar for all configurations (and is thus visible in Fig. 10 for the conformal, 0  $\mu\text{m}$  curvature configuration), and is not shown here to preserve the figure's legibility.

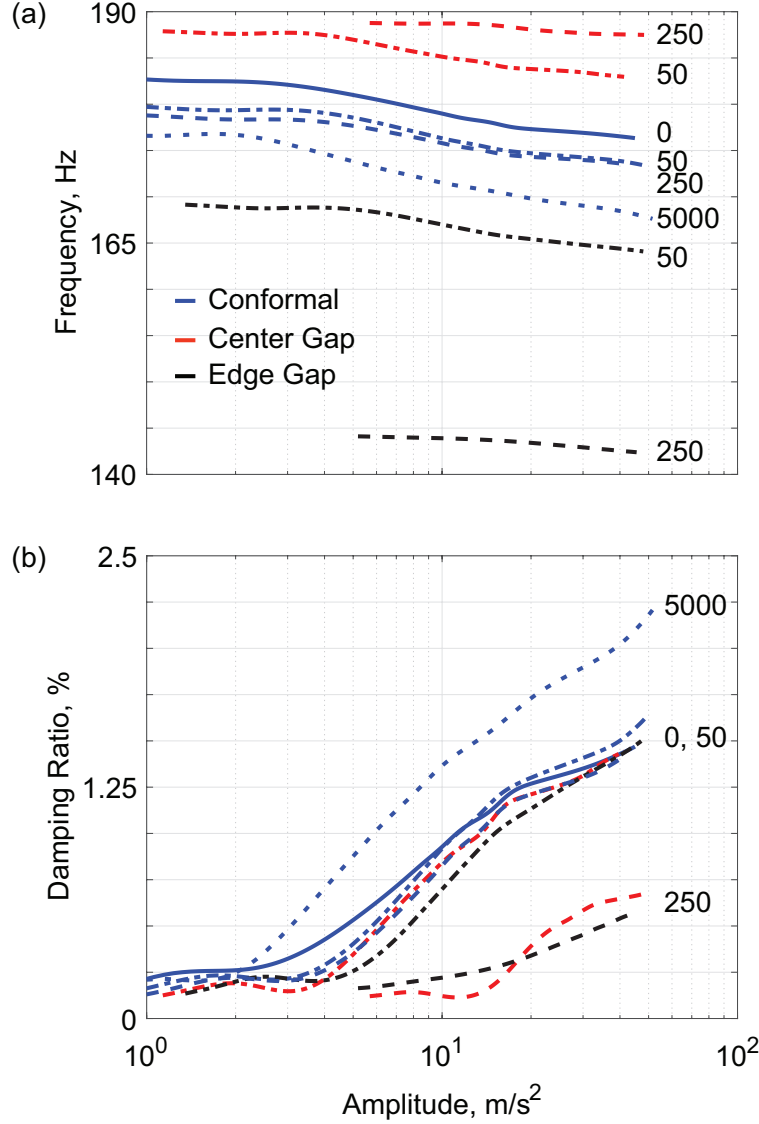


Figure 15: The amplitude dependent (a) resonant frequency and (b) damping ratio for the first mode of the systems with curved interfaces. Blue lines indicate conformal contact, red lines indicate center gap configurations, and black lines indicate edge gap configurations; (—) indicates 0 curvature, (— · —) indicates 50  $\mu\text{m}$  curvature, (— —) indicates 250  $\mu\text{m}$  curvature, and (···) indicates 5000  $\mu\text{m}$  curvature.

For the conformal interfaces, as the curvature was increased from 0  $\mu\text{m}$  to 5000  $\mu\text{m}$ , the natural frequency decreased approximately 5%, and the damping ratio increased approximately 50%. The changes in the dynamic properties were not linearly proportional to changes in interface curvature, however. In terms of the natural frequencies, both the 50  $\mu\text{m}$  and the 250  $\mu\text{m}$  curvatures exhibit a 2% decrease from the 0  $\mu\text{m}$  curvature. Further, the damping ratios for the 0  $\mu\text{m}$ , 50  $\mu\text{m}$ , and 250  $\mu\text{m}$  cases are all similar with only the 5000  $\mu\text{m}$  curvature exhibiting a significant increase.

For the non-conformal interfaces, the introduction of even a small gap (such as the 50  $\mu\text{m}$  case) resulted in a significant change to the natural frequencies. The presence of a center gap stiffened the system, and an edge gap softened the system. Physically, this makes sense as center gaps result in point contact within the interface, which would remove the flexibility observed in the opening and closing of the joint (Brons et al., 2019). Conversely, the presence of an edge gap changes the contact from receding to something similar to Hertzian. Of note, the damping ratios for the non-conformal interfaces are not significantly affected by small interface curvatures, but larger curvatures (such as the 250  $\mu\text{m}$  case) result in significantly reduced (approximately 60% reduced) damping ratios for both edge and center gap configurations.

Taken together with the analysis of the variability and repeatability due to the roughness of the interface, these results imply that deviations from parallelism (i.e. that the two sides of an interface are parallel and conforming) can significantly change the dynamic response of a jointed structure. This leads to the Variability Hypothesis for joint mechanics:

**The Variability Hypothesis** states that the part-to-part variability for nominally identical specimen can be attributed to differences in the meso-scale geometry and roughness of the interface.

A consequence of this hypothesis would be that detailed knowledge of the grain structure, precise position of asperities, or other sub-micron features that would be prohibitively expensive to control for in manufacturing is not necessary to understand (and ultimately predict) the nonlinear response of a jointed structure. This consequence has already found partial support in a recent study using finite element models of the linearized mode shapes of a jointed structure and the simulated contact pressure distribution within an interface to predict the nonlinear dynamic properties of an assembly (Rojas et al., 2019). Without considering the interface roughness and meso-scale structure, (Rojas et al., 2019) found that approximately 85% of the stiffness nonlinearity and 55% of the damping

nonlinearity could be predicted by the simplified finite element simulations (i.e. the linearized modal analysis with the interface stuck together, and a static nonlinear contact pressure calculation). Of note, the intention of the work was to use easy to simulate models instead of a full, nonlinear model of an interface, in order to make meaningful predictions about the potential nonlinearity in a system.

### 6.3. Macro-Scale Interface Variations

To gain further insights into the importance of the contact patch, four perturbations of the nominal system (Fig. 3 and Fig. 16(e)) were designed to address two different notions from recent research.

The first redesign is based on findings in the solid mechanics literature in which it is observed that a traditional lap joint, which is a form of receding contact, is a poor design choice due to fretting-related issues (Hills et al., 2013). Receding contacts in lap joints are characterized by having a loss of contact near the edges as bending stresses lead to the separation of the two sides of the interface<sup>7</sup>. For incomplete contact, such as Hertzian contact or contact between two cylinders, the contact area is a function of the applied normal load, and the contact pressure smoothly tends to zero as the contact edge is approached (Barber et al., 2008). This notion led to the design of the Hertzian interface (Fig. 16(a)), which consists of four cylindrical bumps that are designed to not yield under the nominal bolt torques used in experiments.

The second set of redesigns is based on recent research within the structural dynamics community that indicates that most of the dissipation within a jointed interface occurs away from the pressure cones of the bolts (Goyder et al., 2013, 2014, 2015; Dossogne et al., 2017). Therefore, the second perturbation (Fig. 16(b), hereafter referred to as the small pad), is designed to only have contact directly under the pressure cones of the bolts. If most of the energy is dissipated in the area farthest away from the bolt locations, then removing contact in that region should reduce uncertainty in the response and increase repeatability due to less frictional dissipation occurring. To explore the transition between the small pad interface and the nominal, flat interface, a large pad (Fig. 16(c)) is designed as a third perturbation. Additionally, the inverse of the large pad

---

<sup>7</sup>By contrast, if the lap joint was loaded across the entirety of its outer surface, it would be a complete contact that is characterized by a sharp edge in its profile, which results in the contact area being independent of the magnitude of the normal load. Additionally, sharp edge contact often gives rise to singularities in the stress distributions (Churchman and Hills, 2006).

(termed the reverse pad) is designed to see if this significantly exacerbates the dynamics of the system, Fig. 16(d), since contact only occurs outside of the frustum of the bolts.

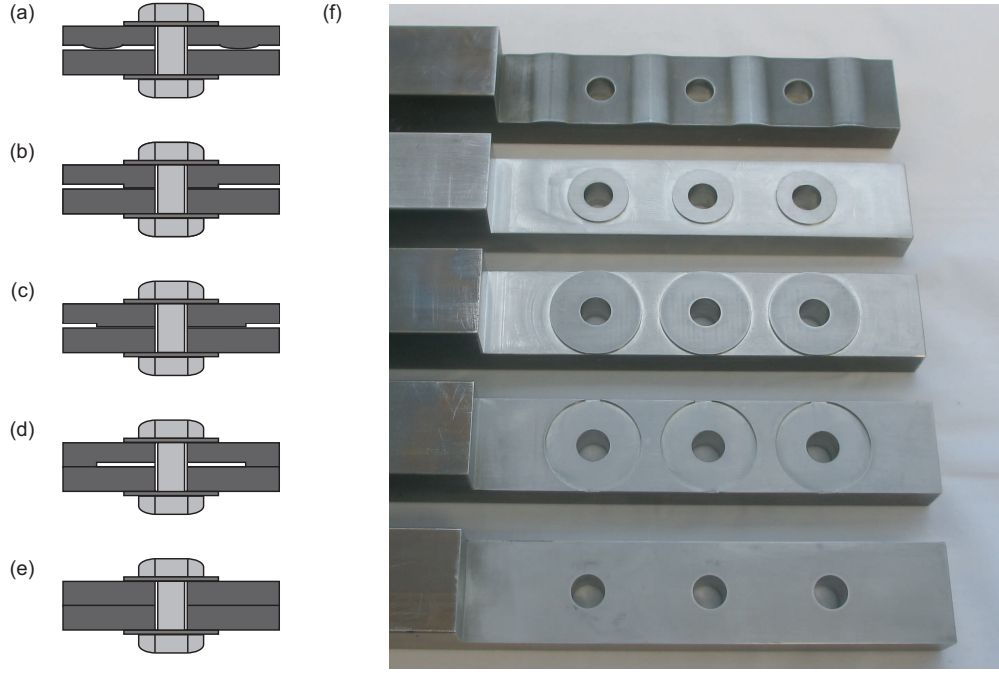


Figure 16: Modifications of the interface of the Brake-Reuß beam showing profiles of the (a) Hertzian contact, (b) small pad, (c) large pad, (d) reverse pad, (e) nominal system, and (f) photo of the five different interfaces.

#### 6.4. Influence of Macro-Scale Interface Variations on Variability and Repeatability

The dynamics of the nominal system, measured by impact hammer excitation, are shown in Fig. 17 as the results of 45 separate measurements, including three assemblies of the same system, three different impact levels, and five repetitions of each impact level for each assembly. In all measurements, the bolts are tightened to 20 Nm as detailed in Section 3.4. Figure 17 shows four different aspects of the system. Subplot (a) shows the frequency response of the system and the response filtered about the first natural frequency for multiple excitation forces. The amplitude of the ringdown response (calculated by applying the Hilbert transform (Sumali and Kellogg, 2011) to the filtered data and then fitting a polynomial function to the resulting amplitude) is shown in subplot (d). From this fit, the amplitude dependent natural frequency (subplot (b)) and amplitude dependent damping ratio (subplot (c)) are extracted. In what follows, only the first mode is highlighted for brevity, though similar trends are observed for the higher modes. For the amplitude dependent frequency and damping ratio of the first mode (Figs. 17(b) and (c)), the

repeatability is observed as the width of the collection of measurements at a given amplitude of response acceleration. For both this and the subsequent systems, the high, medium, and low impact responses lie mostly on top of each other (with the exception of subplot d, which had an initial amplitude level that is directly dependent on the impact magnitude). This is indicative that there is both low modal coupling (if any) and high repeatability.

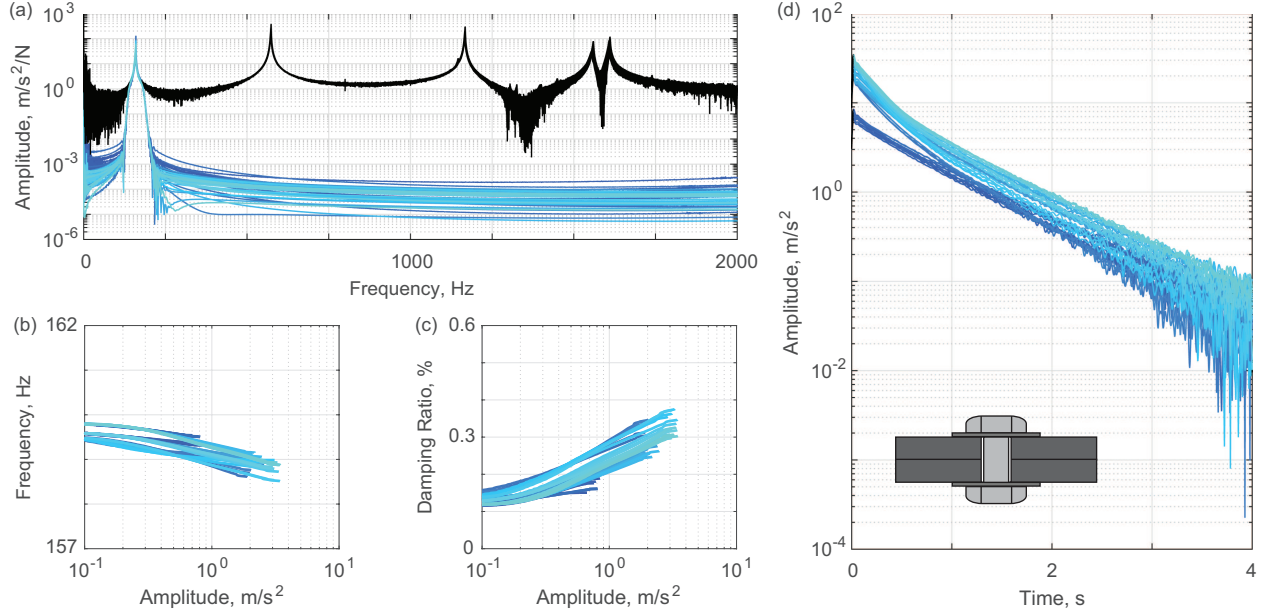


Figure 17: For the nominal system with bolts tightened to a preload of 20 Nm and excited by an impact hammer, shown are the (a) frequency response function and modally filtered response, (b) amplitude dependent frequency, (c) amplitude dependent damping, and (d) envelope of decay of transient ringdown. Light blue curves indicate high level impact tests, and dark blue curves indicate low level impact tests. The inset in (d) shows the interface geometry for these results.

In Fig. 17(d), the magnitude of the response envelope of the transient ringdown is shown. If the system is damped by pure Coulomb damping, then the windowed response would be an exponential decay in this semi-log scale until the noise threshold is reached (at approximately 2 to 4 seconds in the following sets of experiments). On the other hand, if the response is dominated by linear, viscous damping, the windowed response would be best fit by a straight line in this semi-log scale. For the nominal system, the response conforms to neither that of Coulomb dry friction nor linear viscous damping, but rather some intermediate value. This is typical of jointed systems, and has been extensively reported previously (Segalman et al., 2009; Brake, 2017; Segalman, 2005).

By contrast to the nominal system, the dynamics of the small pad system (shown in Fig. 18)

exhibit nearly linear behavior over the excitation range studied. There is almost no discernible change in frequency or damping ratio (Figs. 18(b) and (c), respectively). Further, the envelope of the ringdown response appears as a straight line in Fig. 18(d) (implying linear, viscous damping). the repeatability of the small pad system is significantly higher than the nominal system, as is evident in comparing Figs. 18 (b) and (c) to Figs. 17 (b) and (c). These results are summarized in Table 2. The frequency repeatability range is defined as the absolute deviation of the responses in the amplitude dependent frequency at a fixed amplitude (the amplitude is chosen to maximize the frequency repeatability range), and the damping repeatability range is likewise defined as the absolute deviation of the damping ratios in the amplitude dependent damping ratio. The small pad system is designed to only have contact directly under the pressure cone of the bolts. The rationale behind this design choice is that this system will have a nearly constant and high contact pressure, minimizing the amount of microslip that occurs (this is also evident by the damping ratio being close to the material damping value of 0.05% and no amplitude dependence of frequency or damping). Measurements confirm that the contact pressure for the small pad system is nearly uniform (Dossogne et al., 2017).

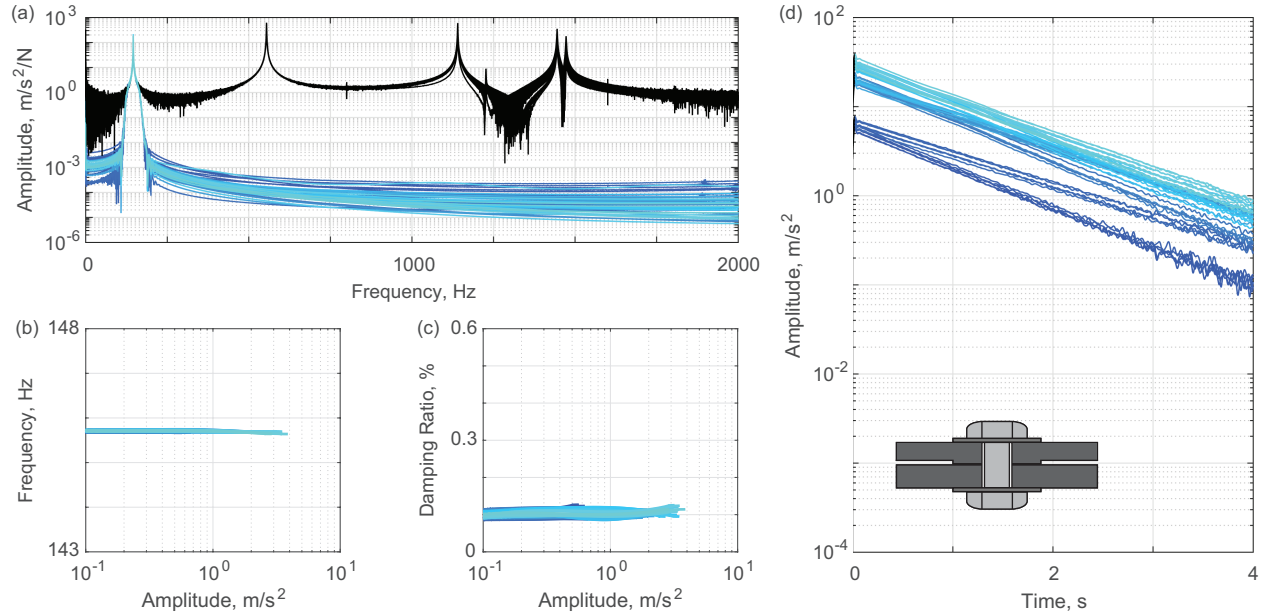


Figure 18: For the small pad system with bolts tightened to a preload of 20 Nm and excited by an impact hammer, shown are the (a) frequency response function and modally filtered response, (b) amplitude dependent frequency, (c) amplitude dependent damping, and (d) envelope of decay of transient ringdown. The inset in (d) shows the interface geometry for these results.

The large pad system is intended to be an intermediate interface between the nominal system and the small pad system. The contact pads are designed to be twice the radius of the contact pads of the small pad system, as shown in Fig. 16. Figure 19 shows that the variability of the large pad system is lower than for the nominal system, but significantly higher than the small pad system. Further, due to the increased contact area (and therefore increased energy dissipation during dynamic excitation), the response is once more nonlinear (i.e. the non-flat curves of Figs. 19(b) and (c)).

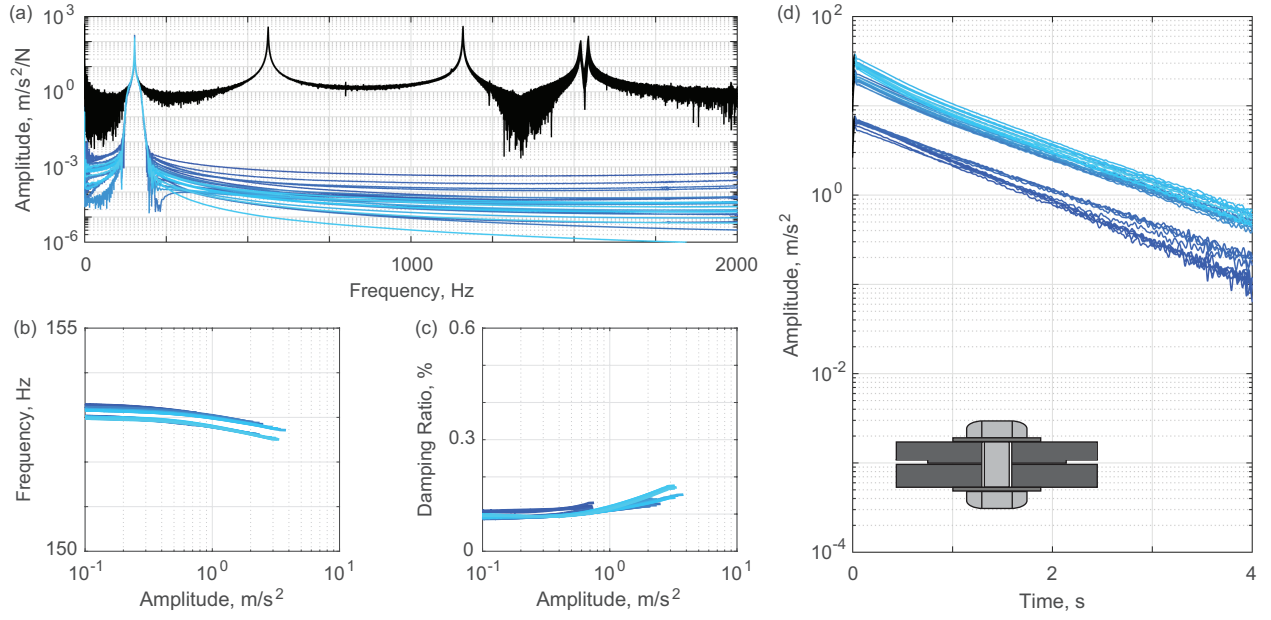


Figure 19: For the large pad system with bolts tightened to a preload of 20 Nm and excited by an impact hammer, shown are the (a) frequency response function and modally filtered response, (b) amplitude dependent frequency, (c) amplitude dependent damping, and (d) envelope of decay of transient ringdown. The inset in (d) shows the interface geometry for these results.

The reverse pad system is designed to only have contact *away* from the pressure cone of the bolts. Consequently, the contact pressure is lower than the small pad system, except near the edges of the interface where sharp edge contact is present, and there are large portions of the interface with close to zero contact pressure. The resulting dynamics (Fig. 20) show the lowest repeatability of all of the interfaces measured, and no clear trends in the amplitude dependent frequency (Fig. 20(b)).

The final interface geometry is the Hertzian contact system, with dynamics shown in Fig. 21. The contact pressure for the Hertzian contact system is uniform and high, similar to the small pad system. However, the contact force supported by the Hertzian contact system is measured to be

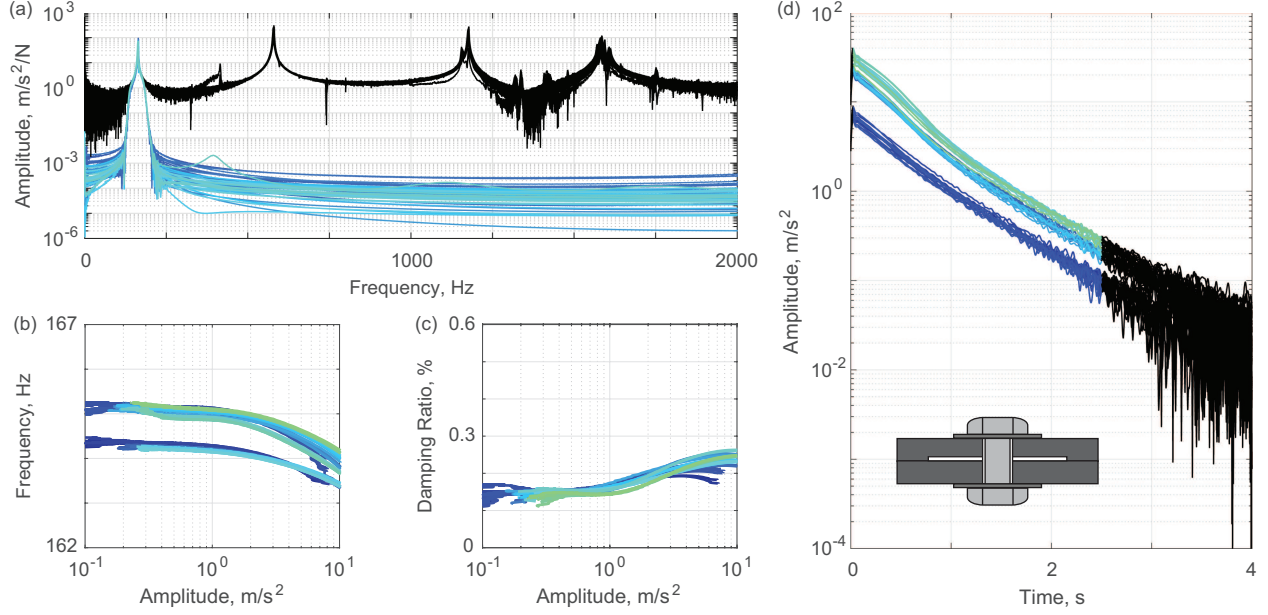


Figure 20: For the reverse pad system with bolts tightened to a preload of 20 Nm and excited by an impact hammer, shown are the (a) frequency response function and modally filtered response, (b) amplitude dependent frequency, (c) amplitude dependent damping, and (d) envelope of decay of transient ringdown. Due to the high level of noise, only the first 2.5 seconds of response are used for the Hilbert transform. The inset in (d) shows the interface geometry for these results.

significantly lower than for the small pad system, due to the reduced contact area, which indicates that more of the load is carried by the bolt for this interface than in other interfaces. As a result, the system exhibits a small deviation from being linear (as is evidenced in Figs. 21(b)-(d)).

Table 2 further summarizes the contact pressure and area. These statistics are calculated from a digitization of measurements made with both static contact pressure films and an electronic pressure film system. This set of statistics - maximum, mean, standard deviation, and kurtosis - have been found to be statistically significant for estimating both stiffness and damping nonlinearities in jointed structures (Rojas et al., 2019); whereas other statistics, such as skewness, were found to be statistically insignificant. As noted in the table, it is likely that three of the pressure measurements were saturated, resulting in the peak pressures (and other statistics) not being accurately measured. In particular, saturation affects the Hertzian interface the most, followed by the small pad interface, and the reverse pad interface. Nonetheless, the trends shown here are reflective of the qualitative results (shown in Fig. 22) and are useful for developing insights into the interfacial physics. One consideration for using static pressure film is that the contact pressures and contact area are over

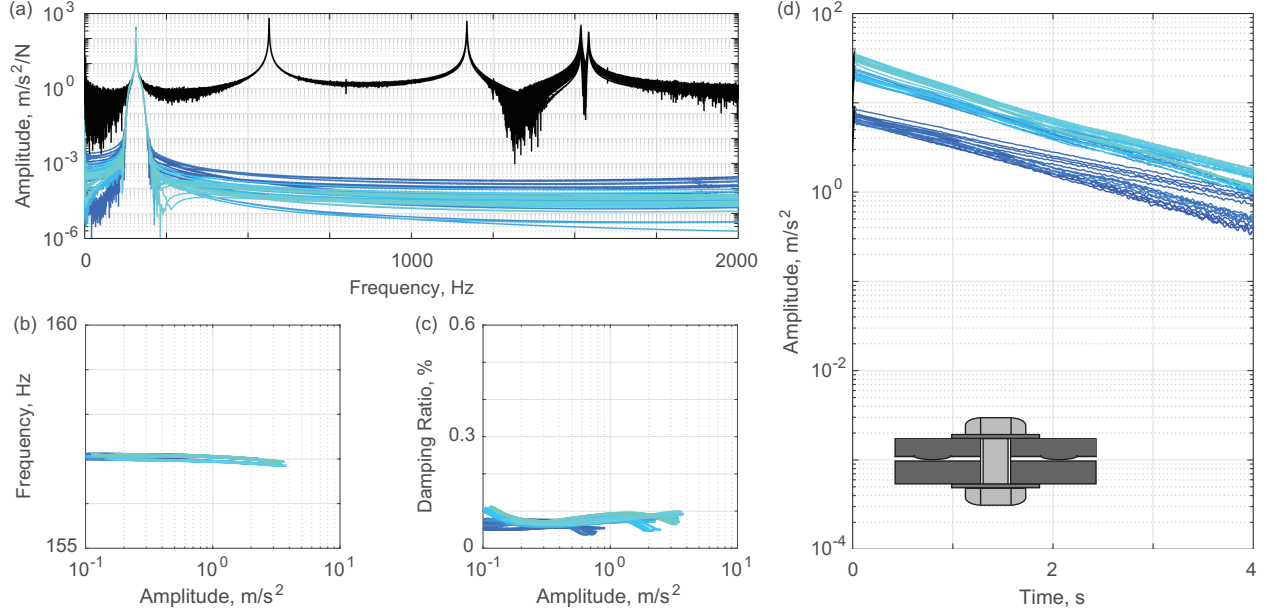


Figure 21: For the Hertzian contact system with bolts tightened to a preload of 20 Nm and excited by an impact hammer, shown are the (a) frequency response function and modally filtered response, (b) amplitude dependent frequency, (c) amplitude dependent damping, and (d) envelope of decay of transient ringdown. The inset in (d) shows the interface geometry for these results.

estimated by static films due to beam bending effects - as the bolt torques are increased from 0 to 20 Nm, the two sides of the interface separate in low contact pressure areas near the periphery (see, for instance, (Brons et al., 2019)).

### 6.5. Discussion of Interface Modifications

These observations, taken together with the observations from the influence of roughness on repeatability and variability in the previous section, compliment the observations made in (Goyder et al., 2013, 2014, 2015; Dossogne et al., 2017) that indicate that most of the dissipation within an interface occurs away from the frustum of the bolts. In these regions away from the bolts, the contact pressure tends to be low and the threshold for microslip is reduced. This set of observations thus leads to the Dissipation Hypothesis for joint mechanics:

**The Dissipation Hypothesis** states that the low (but non-zero) contact pressure regions in an interface are the location of energy dissipation in measurements.

There is an important distinction between the Dissipation Hypothesis and the findings of (Goyder et al., 2013, 2014, 2015): the hypothesis implies that dissipation occurs at a transitionary

	Nominal	Small Pad	Large Pad	Reverse Pad	Hertzian
Maximum Pressure (MPa)	49.7	79.2*	65.2	79.2*	79.2*
Mean Pressure (MPa)	23.8	62.4	36.1	45.9	37.0
Standard Deviation (MPa)	11.0	24.9	15.3	31.8	19.9
Kurtosis (MPa)	2.09	2.62	2.36	1.18	2.45
Contact Area (cm <sup>2</sup> )	21.6	6.65	14.1	12.2	3.03
Frequency Shift (Hz)	1.4	0.1	0.5	3.6	0.2
Damping Ratio Shift (%)	0.26	0.03	0.08	0.13	0.03
Frequency Repeatability (Hz)	0.5	0.08	0.3	1.1	0.1
Damping Repeatability (%)	0.16	0.03	0.03	0.04	0.03

Table 2: Measured interface properties from static measurements using contact pressure film and amplitude dependent properties from ringdown measurements spanning acceleration amplitudes from 4 m/s<sup>2</sup> to 0.1 m/s<sup>2</sup>. Note, \* indicates that a value is likely lower than in actuality due to saturation of the pressure films.

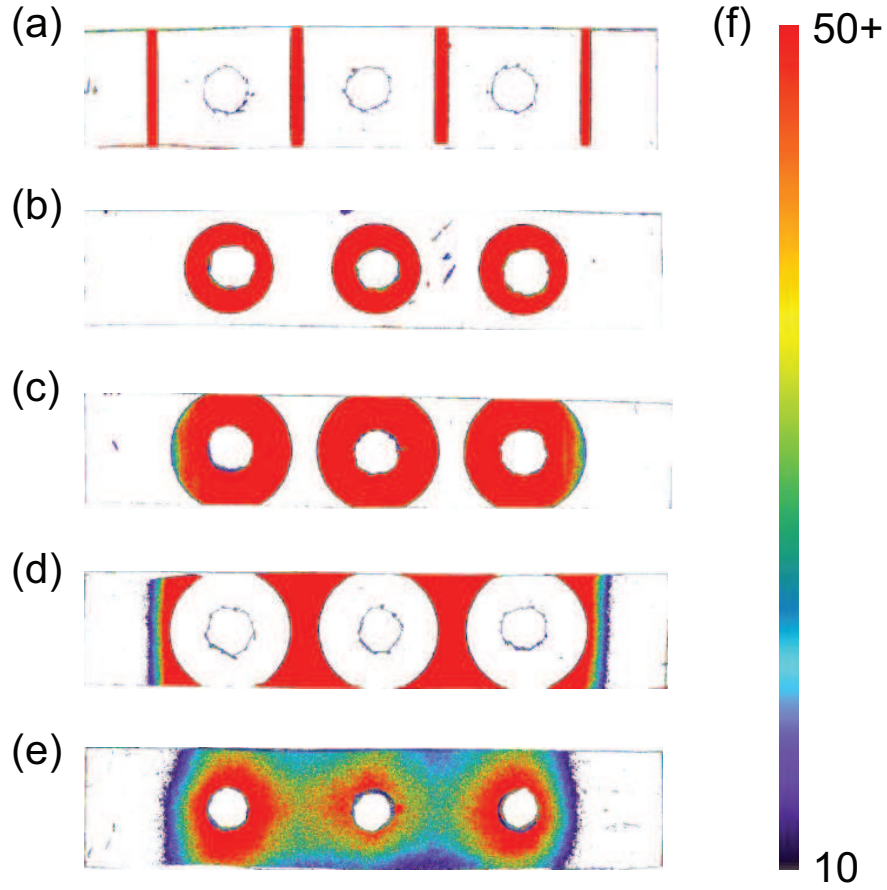


Figure 22: Digitized static contact pressure film measurements made for the five different macro-scale interface variations: (a) the Hertzian interface, (b) the small pad interface, (c) the large pad interface, (d) the reverse pad interface, (e) the nominal (flat) interface, and (f) contact pressure magnitude in MPa.

region from high to low contact pressure inside of a joint, whereas (Goyder et al., 2013, 2014, 2015) implies that dissipation occurs at an unspecified location away from the frustum of the bolts. This is important because the distinction specifies precisely where energy is dissipated and thus can be used to guide approaches to redesign a joint to change its dissipative characteristics. By designing the interface such that there are only high contact pressure regions (such as for the small pad, Hertzian, or non-conformal systems), the damping nonlinearity is observed to significantly decrease. Further, the stiffness nonlinearity is also observed to decrease such that, in the extreme case of the small pad and Hertzian contact, the dynamics of the system appear to be linear. By removing the regions of low contact pressure from the interface, two aspects of the contact change: first, the threshold for dissipation due to microslip is increased (since, according to the Coulomb friction model, frictional force is linearly proportional to the normal force), and second, the potential for impact dissipation is decreased (see (Seeger et al., 2018; Brons et al., 2019) for detailed inspection of impact nonlinearities in bolted joints).

## **7. Influences of the Far-Field Structure on the Response of Nominally Identical Interfaces**

In previous sections, the effect of modifying the interface (whether through geometric changes, roughness changes, or alignment changes) was discussed. In this section, the effect of changing the far-field structure (i.e., the structure around the joint) is presented. As the far-field structure is modified, the loading of the joint is changed for identical excitations. That is, by changing the far-field structure, the mode shapes of the beam are changed sufficiently to significantly modify the stresses in the joint. As a result, the nonlinearity in each of the systems is hypothesized to be engaged to a different degree when each of the systems is excited with the same modal force. This hypothesis is extrapolated from (Do and Ferri, 2005, 2008), which investigated how the dissipative properties of a system changed as the mass and stiffness properties of the system were modified while keeping the viscous or frictional properties constant.

### *7.1. Far-Field Geometry Variations*

Three different systems are considered, each having a geometrically identical interface. The first system is the nominal Brake-Reuß beam (Fig. 3 and Fig. 23(a)), which is the reference system for all experiments. The second system contains a stiffness modification that significantly lowers the stiffness of the beam away from the interface (Fig. 23(b)), hereafter termed the spring beam.

The third system significantly increases the mass (and stiffness, thus affecting the mode shapes) of the system by increasing the length of the beam by 50% (Fig. 23(c)). For each of these three systems, the geometry of the interface is identical; it is only the far-field structure that is modified. The intention of these design modifications was to study how the dynamic response of the assembly changed due to modifications in the structure supporting the jointed interface while leaving the interface the same in each design. Previous research on discrete mass systems showed that by tuning the support structure around a frictional interface, the apparent behavior of the nonlinearity could be changed from an energy pump, in which energy is transferred from the low frequency modes of one substructure to the high frequency modes of the second substructure, to a locked system in which the joint dissipates no energy (Do and Ferri, 2005). If this result was generalizable to a real system, then that would imply that an alternative approach to reduce the uncertainty in a jointed structure would be to redesign the support structure around the joint in order to change the manner in which the joint is loaded/excited.

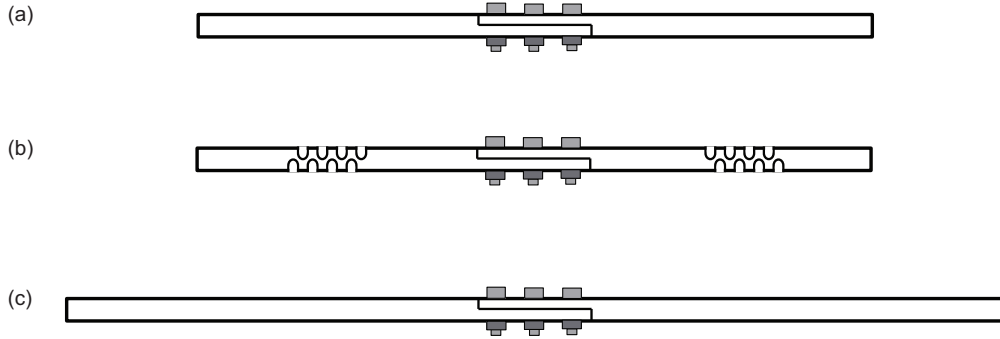


Figure 23: Modifications of the far-field structure of the Brake-Reuß beam showing the (a) nominal system, (b) stiffness modified (spring) system, and (c) length modified (long) system.

## 7.2. Influence of Far-Field Geometry Variations on Measured Dynamic Properties

For measuring the dynamic properties of each system, the bolts were tightened to 20 Nm, and Procedure 3I was used for measuring the dynamic properties (Cooper et al., 2017). Compared to the nominal system (Fig. 17), the spring beam exhibits a lower dependence of natural frequency and damping ratio on excitation amplitude (as shown in Fig. 24). By contrast, the long beam exhibits higher dependence of natural frequency and damping ratio on excitation amplitude (as shown in Fig. 25). That is, despite the interface being nominally identical in geometry for each of the three systems, the measured dynamic properties appear significantly different. This result is explained

by analyzing the mode shapes of the three beams (Fig. 26). For the spring beam, much of the strain energy of the beam is stored in the spring-like section where material has been removed from each beam. Consequently, the amount that the beam is strained at the location of the interface is lower, resulting in lower stresses and less relative motion. By contrast, both the nominal beam and the long beam exhibit the greatest amount of curvature in their first mode at the interface location, which implies that the stresses across the interface is higher. **Thus, even though the three beams have nominally identical joints, the manner in which the joints are loaded give rise to different *apparent* joint properties when a joint model is calibrated to the experimental data**, such as in (Cooper et al., 2017; Balaji and Brake, Under Review).

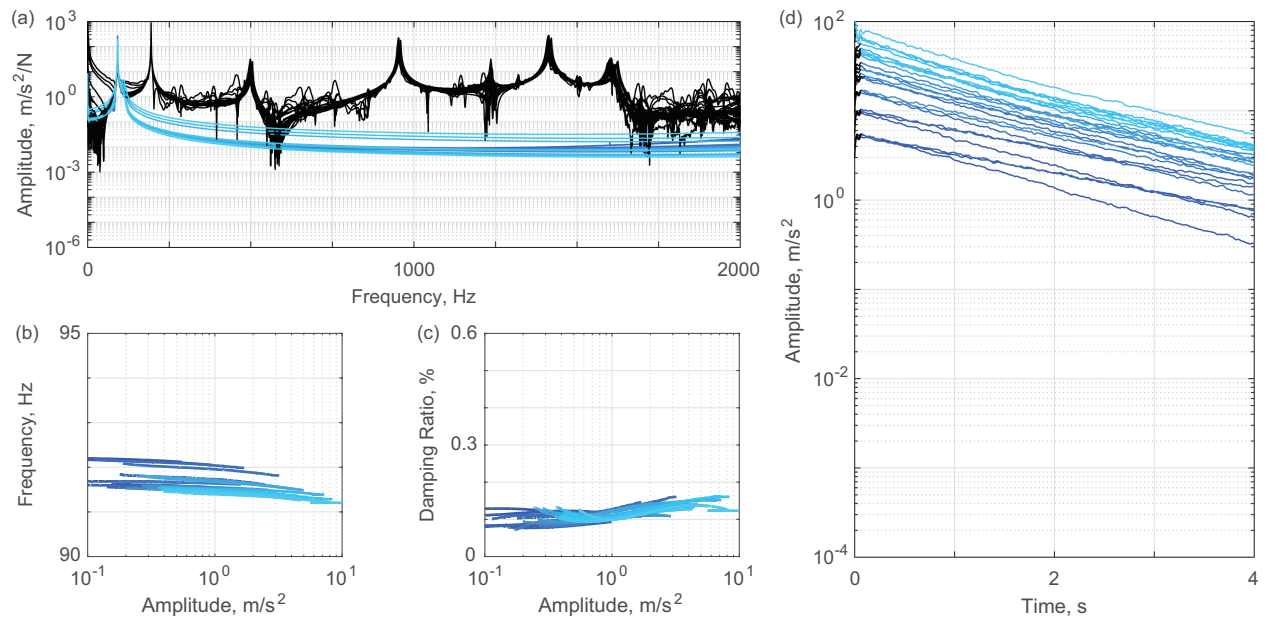


Figure 24: For the spring system with bolts tightened to a preload of 20 Nm and excited by an impact hammer, shown are the (a) frequency response function and modally filtered response, (b) amplitude dependent frequency, (c) amplitude dependent damping, and (d) envelope of decay of transient ringdown.

In the numerical analysis of these three systems (Balaji and Brake, Under Review), it was shown that discrete (as opposed to modal) interface models calibrated to the experimental data set from the nominal system are able to predict both the nonlinear stiffness and nonlinear damping properties of both the long beam and the spring beam. Thus, if a joint is modeled in a discrete manner, then it is possible to predict the behavior of a joint in a new structure using data from a system that is easier to model and easier to fabricate. See the numerical analysis of (Balaji and

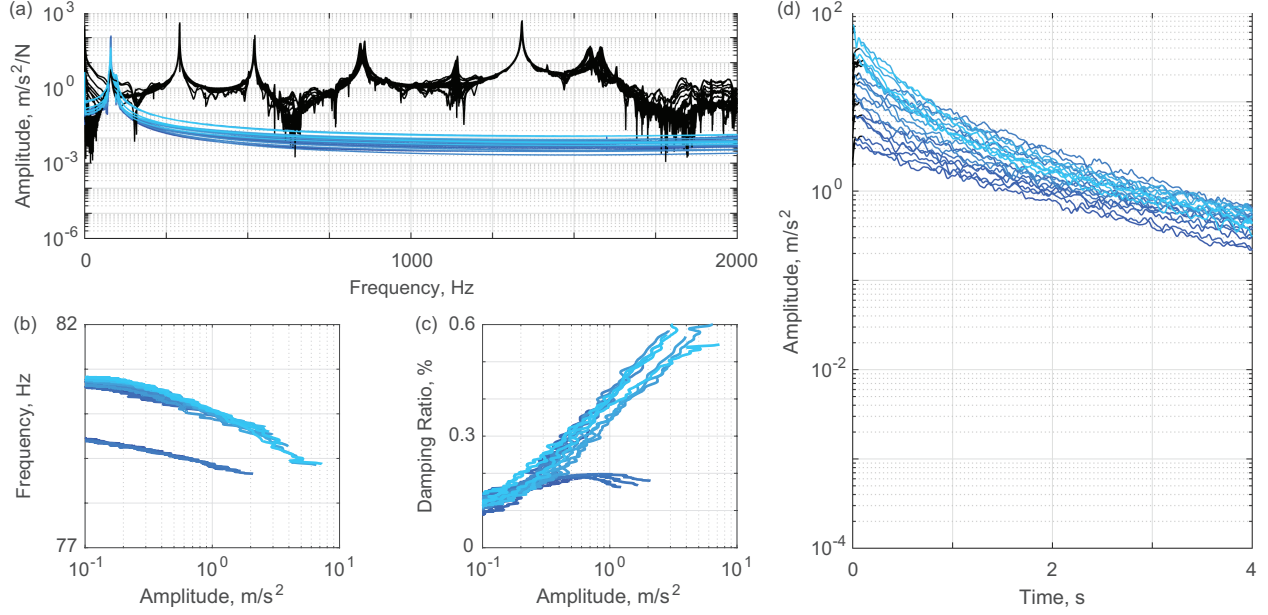


Figure 25: For the long system with bolts tightened to a preload of 20 Nm and excited by an impact hammer, shown are the (a) frequency response function and modally filtered response, (b) amplitude dependent frequency, (c) amplitude dependent damping, and (d) envelope of decay of transient ringdown.

Brake, Under Review) for more details.

## 8. Discussion

The focus of the experiments described in this paper was on the potential sources of uncertainty in the form of variability and lack of repeatability. To minimize the uncertainty in the measurements, several sets of factors were identified. First, having a formal procedure for assembling the systems was paramount for repeatability. This procedure needed to account for not only bolt tightening orders but also the precise alignment of the interface. Through the use of straight beams and shims to assist with the alignment, the observed variation in the natural frequencies for low amplitude excitation was decreased from 5.6% to 0.063%, approximately two orders of magnitude. This difference was mediated by the preload of the system; consistent with other observations in the literature, the preload is directly related to the repeatability of measurements of jointed properties with higher preloads yielding more repeatable measurements. Further, with a formal procedure for measurements established, the part-to-part variability was significantly reduced once the roughness and meso-scale geometry of the interface was controlled for. This implies that non-linear characteristics of a jointed structure are primarily due to features that are reasonable to

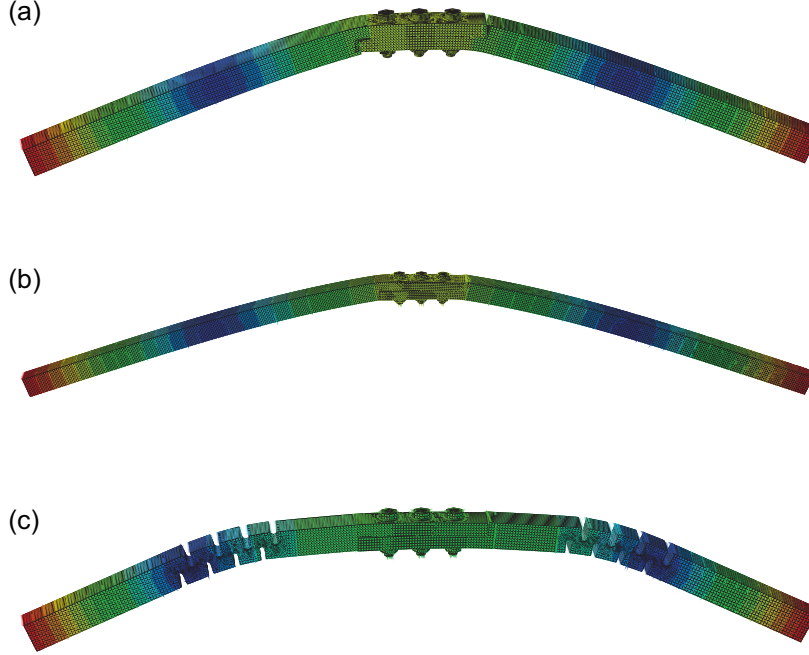


Figure 26: Numerical predictions of the first bending mode for the (a) nominal system, (b) long system, and (c) spring system.

control in manufacturing (i.e. roughness, meso-scale curvature, and larger scale criteria). This is a serendipitous finding as it further implies that a predictive joint model will not need to include sub-micron and nano-scale features.

Second, the contact pressure was found to be a key metric in assessing the repeatability and linearity of the interface. Together with the observations made during *in situ* measurements of contact pressure (Brake et al., 2017; Seeger et al., 2018), it was observed that assemblies that had high, uniform interfacial contact pressures were more robust to sources of uncertainty. In particular, assemblies with rough interfaces at the joint location tended to exhibit more uncertainty in the measurements of the dynamic properties of the jointed system than assemblies with smooth interfaces. This is consistent with the previously reported results (Fig. 1 and (Segalman et al., 2009; Wang and Mignolet, 2014; Brake, 2017)). Interface modifications such as machining features, curvature/warping at the meso- and micro-scales, and deformations due to residual stresses accumulated through the manufacturing process were the major source of variability in comparing two nominally identical systems. In studying the influence of meso-scale curvatures on the dynamics of the jointed structure, even curvatures as small as  $50\text{ }\mu\text{m}$  led to changes in resonant frequency of

approximately 6% (though the changes in damping were significantly smaller).

Third, the contact pressure in the interface and dynamic properties of the system can be directly modified by changing the interface geometry. When the geometry is changed to have high, uniform areas of contact pressure and no areas with low (but non-zero) contact pressures, the measurements of the assemblies exhibited higher repeatability and, in some cases, were linear over the range of excitations studied (such as the small pad interface discussed in Section 6). Once areas with low contact pressure were introduced to the system, the potential for microslip greatly increased, which, in turn, resulted in a stronger nonlinearity.

From these observations, the recommendation for reducing uncertainty in experiments on bolted joint mechanics is to have a mechanism to repeatedly align (or self-align) the interface, to control for the bolt tightening order (and to use the industry practice of tightening part way first for each bolt then fully), to use a highly polished interface if possible, and to design the interface to only have high contact pressure regions. Future work should focus on the influences of using polymer/elastomer gaskets for applications that require that the interface provides some amount of sealing. In preliminary analyses, the introduction of polymeric material to the interface results in slightly more linear dynamics (Seeger et al., 2018).

Lastly, even when the joint itself is non-ideal from the above perspective, it is still possible to make it appear linear by modifying the support structure around the joint. If the mode shapes of the system can be modified such that the joint is not exercised, then the potential for microslip is reduced, resulting in a more linear response.

## 9. Conclusions

This paper has summarized and presented a four-year long testing program in which the dynamics of the Brake-Reuß beam were investigated. A nominal version of the Brake-Reuß beam was proposed as a benchmark system for studying joint mechanics. The Brake-Reuß beam was used to assess how the experimental setup and the roughness of the interface influenced the nonlinear dynamics of the system, the uncertainty attributed to variability and repeatability, and the role of settling and wear. To study the jointed system, a Tribomechadynamics approach was adopted in which the dynamics, contact mechanics, and tribological properties of the system were all considered. Once the nominal system was sufficiently characterized, modifications were made to assess the role that interface geometry (as a proxy for contact pressure) and the surrounding support

structure (as a proxy for modal forces) had on the response of the assembled system. Specific conclusions from this series of measurements follow:

- By redesigning the interface to only have regions of high contact pressure, the dynamics of the assembled system appear linear as the force needed to initiate microslip was significantly higher than tested.
- Interfaces with higher roughnesses have been observed to have significantly different contact patches than interfaces with low roughness. For high roughness interfaces, the regions of high contact pressure are localized around the bolt holes and most of the interface is characterized by low contact pressure. For low roughness interfaces, the contact pressure is more evenly distributed across the entire interface. Further, interfaces with lower surface roughness results in higher repeatability and lower sensitivity to bolt tightening orders and bolt preloads than interfaces with higher surface roughness. This indicates that lower surface roughness interfaces help ameliorate the uncertainty due to bolt torque levels.
- The manner in which the interface is loaded (e.g. the mode shapes) has significant effect on the apparent nonlinear properties of the joint. When the modes of vibration do not exercise the joint, the modal properties will be more linear than when the modes of vibration have high modal strain at the joint location. Thus, a joint can be linearized not only through changing its physical geometry, but also by changing the structure around it such that it is not exercised by the dominant modes of the system.
- The assembly procedure is paramount to ensure repeatability in results. When measurements of the linear regime of the system exhibit high uncertainty (i.e. high variability or low repeatability), the experimental setup should be carefully inspected to ensure that it is not introducing unintended uncertainty into the system. Without thorough control of the assembly procedure, the measured uncertainty can be much greater than the frequency shifts due to the nonlinearity of the jointed interface.
- Even in low cycle loading scenarios, wear and fretting can be observed if there are regions of low contact pressure in the interface. As damage is accumulated in the system, the linear frequencies of the system often decrease. Thus, a potential metric to study accumulated damage may be the change in linear natural frequencies of the system.

- If a stochastic model of the system is more important than precisely understanding the nonlinearities in the system, then introducing uncertainty through the experimental setup could potentially span the range of the nonlinear responses of the system. Caution with this approach is advised, though, as it has only been demonstrated on the present system.

## Acknowledgements

The authors would like to thank the participants of the Nonlinear Mechanics and Dynamics (NOMAD) Research Institute where much of this work was completed between the summers of 2014 and 2016. The NOMAD Research Institute is a multinational research activity that is sponsored by Sandia National Laboratories and hosted at the University of New Mexico. Sandia National Laboratories is a multimission laboratory managed and operated by National Technology and Engineering Solutions of Sandia, LLC., a wholly owned subsidiary of Honeywell International, Inc., for the U.S. Department of Energy's National Nuclear Security Administration under contract DE-NA0003525. The authors would also like to thank the participants of the Nonlinear Dynamics of Coupled Structures and Interfaces (ND-CSI) Research Center where further work was completed during the summer of 2017. The ND-CSI Research Center was hosted at Rice University in 2017, and was supported by a grant given by Rice University. Finally, the authors would also like to thank SIEMENS AG for lending the data acquisition systems used in many of the experiments.

## References

- Allen, M.S., Mayes, R.L., 2010. Estimating degree of nonlinearity in transient responses with zeroed early-time fast fourier transforms. *Mechanical Systems and Signal Processing* 24, 2049–2064.
- Balaji, N.N., Brake, M.R.W., Under Review. The surrogate system hypothesis for joint mechanics. *Mechanical Systems and Signal Processing* .
- Barber, J.R., Klarbring, A., Ciavarella, M., 2008. Shakedown in frictional contact problems for the continuum. *Comptes Rendus Mécanique* 336, 34–41.
- Bonney, M.S., Robertson, B.A., Schempp, F., Brake, M.R.W., Mignolet, M.P., 2016. Experimental determination of frictional interface models, in: 34th International Modal Analysis Conference (IMAC XXXIV), Orlando, FL.

- Brake, M.R., Reuß, P., Segalman, D.J., Gaul, L., 2014. Variability and repeatability of jointed structures with frictional interfaces, in: 32nd International Modal Analysis Conference (IMAC XXXII), Orlando, FL.
- Brake, M.R.W. (Ed.), 2017. The Mechanics of Jointed Structures. Springer.
- Brake, M.R.W., Negus, M.E., Schwingshackl, C.W., Reuß, P., Allen, M.S., 2016. The 2015 Nonlinear Mechanics and Dynamics Research Institute. SAND2016-5695. Sandia National Laboratories, Albuquerque, NM.
- Brake, M.R.W., Reuß, P., Schwingshackl, C.W., Salles, L., Negus, M.E., Peebles, D.E., Mayes, R.L., Bilbao-Ludena, J.C., Bonney, M.S., Catalfamo, S., Gastaldi, C., Groß, J., Lacayo, R.M., Robertson, B.A., Smith, S., Swacek, C., Tiedemann, M., 2015. The 2014 Sandia Nonlinear Mechanics and Dynamics Summer Research Institute. SAND2015-1876. Sandia National Laboratories, Albuquerque, NM.
- Brake, M.R.W., Stark, J.G., Smith, S.A., Lancereau, D.P.T., Jerome, T.W., Dossogne, T., 2017. In situ measurements of contact pressure for jointed interfaces during dynamic loading experiments, in: 35th International Modal Analysis Conference (IMAC XXXV), Garden Grove, CA.
- Brons, M., Klaassen, S., Kasper, T., Chauda, G., Schwingshackl, C.W., Brake, M.R.W., 2019. Die techniques to identify non-linear interface behaviour in a bolted lap joint, in: 37th International Modal Analysis Conference (IMAC XXXVII), Orlando, FL.
- Cabboi, A., Putelat, T., Woodhouse, J., 2016. The frequency response of dynamic friction: Enhanced rate-and-state models. *Journal of the Mechanics and Physics of Solids* 92, 210–236.
- Catalfamo, S., Smith, S.A., Morlock, F., Schwingshackl, C., Reuß, P., Brake, M.R.W., 2016. Effects of experimental methods on the measurement of a nonlinear system, in: 34th International Modal Analysis Conference (IMAC XXXIV), Orlando, FL.
- Churchman, C.M., Hills, D.A., 2006. General results for complete contacts subject to oscillatory shear. *Journal of the Mechanics and Physics of Solids* 54, 1186–1205.
- Cigeroglu, E., An, N., Menq, C.H., 2007. A microslip friction model with normal load variation induced by normal motion. *Nonlinear Dynamics* 50, 609–626.

- Cooper, S.B., Rosatello, M., Mathis, A., Johnson, K., Brake, M.R.W., Allen, M.S., Ferri, A.A., Roettgen, D.R., Pacini, B.R., Mayes, R.L., 2017. Effect of far-field structure on joint properties, in: 35th International Modal Analysis Conference (IMAC XXXV), Garden Grove, CA.
- Do, N., Ferri, A.A., 2005. Energy transfer and dissipation in a three-degree-of-freedom system with Stribeck friction, in: ASME International Mechanical Engineering Congress and Exposition (IMECE), Orlando, FL.
- Do, N., Ferri, A.A., 2008. Properties of energy transfer within a dry friction damped structural system, in: 49th AIAA/ASME/ASCE/AHS/ASC Structures, Structural Dynamics, and Materials Conference, Schaumburg, IL.
- Dossogne, T., Jerome, T.W., Lancerau, D.P.T., Smith, S.A., Brake, M.R.W., Pacini, B.R., Reuss, P., Schwingshackl, C.W., 2017. Experimental assessment of the influence of interface geometries on structural response, in: 35th International Modal Analysis Conference (IMAC XXXV), Garden Grove, CA.
- Dossogne, T., Noël, J.P., Kerschen, G., 2016. Robust subspace identification of a nonlinear satellite using model reduction, in: 34th International Modal Analysis Conference (IMAC XXXIV), Orlando, FL.
- Eriten, M., Polycarpou, A.A., Bergman, L.A., 2011. Surface roughness effects on energy dissipation in fretting contact of nominally flat surfaces. *ASME Journal of Applied Mechanics* 78, Art. 021011.
- Feldman, M., 1994. Non-linear system vibration analysis using Hilbert transform – i. free vibration analysis method ‘Freevib’. *Mechanical Systems and Signal Processing* 8, 119–127.
- Ferri, A.A., 1995. Friction damping and isolation systems. *Journal of Mechanical Design* 117, 196–206.
- Filippi, S., Akay, A., Gola, M.M., 2004. Measurement of tangential contact hysteresis during microslip. *ASME Journal of Tribology* 126, 482–489.
- Flicek, R.C., Hills, D.A., Barber, J.R., Dini, D., 2015. Determination of the shakedown limit for large, discrete frictional systems. *European Journal of Mechanics A - Solids* 49, 242–250.

- Flicek, R.C., Moore, K.J., Castelluccio, G.M., Hammetter, C., Brake, M.R.W., 2016. Stress waves propagating through jointed connections, in: 34th International Modal Analysis Conference (IMAC XXXIV), Orlando, FL.
- Gaul, L., Nitsche, R., 2001. The role of friction in mechanical joints. *ASME Applied Mechanics Reviews* 54, 93–110.
- Gianola, D.S., Warner, D.H., Molinari, J.F., Hemker, K.J., 2006. Increased strain rate sensitivity due to stress-coupled grain growth in nanocrystalline Al. *Scripta Materialia* 55, 649–652.
- Goyder, H.G.D., Ind, P., Brown, D., 2013. Measurement of damping due to bolted joints, in: *ASME International Design Engineering Technical Conferences IDETC/CIE*, Portland, OR.
- Goyder, H.G.D., Ind, P., Brown, D., 2014. Measurement of damping in a chain of bolted joints, in: *ASME International Design Engineering Technical Conferences IDETC/CIE*, Buffalo, NY.
- Goyder, H.G.D., Ind, P., Brown, D., 2015. Damping in a composite beam with a joined interface, in: *ASME International Design Engineering Technical Conferences IDETC/CIE*, Boston, MA.
- Hills, D.A., Flicek, R.C., Dini, D., 2013. Sharp contact corners, fretting and cracks. *Fracture and Structural Integrity* 25, 27–35.
- Kartal, M.E., Mulvihill, D.M., Nowell, D., Hills, D.A., 2011. Measurements of pressure and area dependent tangential contact stiffness between rough surfaces using digital image correlation. *Tribology International* 44, 1188–1198.
- Lacayo, R.M., Pesaresi, L., Fochler, D., Groß, J., Brake, M.R.W., Schwingshackl, C., 2017. A numerical round robin to predict the dynamics of an experimentally-measured brake-reuss beam, in: 35th International Modal Analysis Conference (IMAC XXXV), Garden Grove, CA.
- Lacayo, R.M., Pesaresi, L., Groß, J., Fochler, D., Armand, J., Salles, L., Brake, M.R.W., Schwingshackl, C., Allen, M.S., 2019. Validation and comparison of a time domain approach and a frequency domain approach for nonlinear modeling of structures with bolted joints. *Mechanical Systems and Signal Processing* 114, 413–438.
- Lavella, M., Botto, D., Gola, M.M., 2013. Design of a high-precision, flat-on-flat fretting test apparatus with high temperature capability. *Wear* 302, 1073–1081.

- Lawal, I.G., Shah, S., Gonzalez-Madrid, M., Hu, T., Schwingshackl, C.W., Brake, M.R.W., 2018. The effect of non-flat interfaces on system dynamics, in: 36th International Modal Analysis Conference (IMAC XXXVI), Orlando, FL.
- Müller, M., Ostermeyer, G.P., 2007. Cellular automata method for macroscopic surface and friction dynamics in brake systems. *Tribology International* 40, 942–952.
- Mulvihill, D.M., Kartal, M.E., Nowell, D., Hills, D.A., 2011a. An elastic-plastic asperity interaction model for sliding friction. *Tribology International* 44, 1679–1694.
- Mulvihill, D.M., Kartal, M.E., Olver, A.V., Nowell, D., 2011b. Investigation of non-coulomb friction behaviour in reciprocating sliding. *Wear* 271, 802–816.
- Noël, J.P., Renson, L., Kerschen, G., 2014. Complex dynamics of a nonlinear aerospace structure: Experimental identification and modal interactions. *Journal of Sound and Vibration* 333, 2588–2607.
- Paggi, M., Barber, J.R., 2011. Contact conductance of rough surfaces composed of modified RMD patches. *International Journal of Heat and Mass Transfer* 54, 4664–4672.
- Panzarino, J.F., Pan, Z., Rupert, T.J., 2016. Plasticity-induced restructuring of a nanocrystalline grain boundary network. *Acta Materialia* 120, 1–13.
- Peeters, M., Kerschen, G., Golinval, J.C., 2011a. Dynamic testing of nonlinear vibrating structures using nonlinear normal modes. *Journal of Sound and Vibration* 330, 486–509.
- Peeters, M., Kerschen, G., Golinval, J.C., 2011b. Modal testing of nonlinear vibrating structures based on nonlinear normal modes: Experimental demonstration. *Mechanical Systems and Signal Processing* 25, 1227–1247.
- Pesaresi, L., Salles, L., Green, J.S., Schwingshackl, C.W., 2017. Modelling the nonlinear behaviour of an underplatform damper test rig for turbine applications. *Mechanical Systems and Signal Processing* 85, 662–679.
- Prasad, S.V., Battaile, C.C., Kotula, P.G., 2011. Friction transitions in nanocrystalline nickel. *Scripta Materialia* 64, 729–732.

- Putignano, C., Ciavarella, M., Barber, J.R., 2011. Frictional energy dissipation in contact of nominally flat rough surfaces under harmonically varying loads. *Journal of the Mechanics and Physics of Solids* 59, 2442–2454.
- Ren, F., Bellon, P., Averback, R.S., 2016. Nanoscale self-organization reaction in Cu-Ag alloys subjected to dry sliding and its impact on wear resistance. *Tribology International* 100, 420–429.
- Rojas, E., Punla-Green, S., Broadman, C., Brake, M.R.W., Pacini, B.R., Flicek, R.C., Quinn, D.D., Schwingshackl, C.W., Dodgen, E., 2019. A priori methods to assess the strength of nonlinearities for design applications, in: 37th International Modal Analysis Conference (IMAC XXXVII), Orlando, FL.
- Scheel, M., Kleyman, G., Tatar, A., Brake, M.R.W., Peter, S., Noel, J.P., Allen, M.S., Krack, M., 2018. System identification of jointed structures: Nonlinear modal testing vs. state-space model identification, in: 36rd International Modal Analysis Conference (IMAC XXXVI), Orlando, FL.
- Schwingshackl, C.W., 2017. Identificaiton of reassembly uncertainties for a basic lap joint, in: 35th International Modal Analysis Conference (IMAC XXXV), Garden Grove, CA.
- Schwingshackl, C.W., Petrov, E.P., Ewins, D.J., 2012. Measured and estimated friction interface parameters in a nonlinear dynamic analysis. *Mechanical Systems and Signal Processing* 28, 574–584.
- Seeger, B., Butaud, P., Du, F., Baloglu, V., Brake, M.R.W., Schwingshackl, C.W., 2018. In situ measurements of interfacial contact pressure during impact hammer tests, in: 36rd International Modal Analysis Conference (IMAC XXXVI), Orlando, FL.
- Segalman, D.J., 2005. A four-parameter Iwan model for lap-type joints. *ASME Journal of Applied Mechanics* 72, 752–760.
- Segalman, D.J., Bergman, L.A., Ewins, D.J., 2010. Report on the SNL/AWE/NSF International Workshop on Joint Mechanics, Dartington, United Kingdom, 27-29 April 2009. Technical Report SAND2010-5458. Sandia National Laboratories, Albuquerque, NM.
- Segalman, D.J., Gregory, D.L., Starr, M.J., Resor, B.R., Jew, M.D., Lauffer, J.P., Ames, N.M.,

2009. Handbook on Dynamics of Jointed Structures. Technical Report SAND2009-4164. Sandia National Laboratories, Albuquerque, NM.
- Smith, S.A., Bilbao-Ludena, J.C., Catalfamo, S., Brake, M.R.W., Reuß, P., Schwingshackl, C., 2015. The effects of boundary conditions, measurement techniques, and excitation type on measurements of the properties of mechanical joints, in: 33rd International Modal Analysis Conference (IMAC XXXIV), Orlando, FL.
- Smith, S.A., Brake, M.R.W., Schwingshackl, C.W., Under Review. On the characterization of nonlinearities in assembled systems. *Journal of Sound and Vibration* .
- Starr, M.J., Brake, M.R., Segalman, D.J., Bergman, L.A., Ewins, D.J., 2013. Proceedings of the Third International Workshop on Jointed Structures. Technical Report SAND2013-6655. Sandia National Laboratories, Albuquerque, NM.
- Sumali, H., Kellogg, R.A., 2011. Calculating damping from ring-down using Hilbert transform and curve fitting, in: 4th International Operational Modal Analysis Conference, Istanbul, Turkey.
- Wang, X.Q., Mignolet, M.P., 2014. Stochastic Iwan-type model of a bolted joint: Formulation and identification, in: 32nd International Modal Analysis Conference (IMAC XXXII), Orlando, FL.

## **Appendix: Engineering Drawings of the Brake-Reuß Beam**

From (Brake, 2017), the engineering drawings of the Brake-Reuß beam are provided for those wishing to replicate this benchmark system.

